$[Ca^{2+}]_i$ Oscillations in Sympathetic Neurons: An Experimental Test of a Theoretical Model

D. D. Friel

Department of Neurosciences, Case Western Reserve University, Cleveland, Ohio 44106-4975; and Department of Molecular and Cellular Physiology, Stanford University School of Medicine, Stanford, California 94305-5426 USA

ABSTRACT $[Ca^{2+}]_i$ oscillations have been described in a variety of cells. This study focuses on caffeine-induced $[Ca^{2+}]_i$ oscillations in sympathetic neurons. Previous work has shown that these oscillations require Ca^{2+} entry from the extracellular medium and Ca^{2+}-induced Ca^{2+} release from a caffeine- and ryanodine-sensitive store. The aim of the study was to understand the mechanism responsible for the oscillations. As a starting point, $[Ca^{2+}]_i$ relaxations were examined after membrane depolarization and exposure to caffeine. For both stimuli, post-stimulus relaxations could be described by the sum of two decaying exponential functions, consistent with a one-pool system in which Ca^{2+} transport between compartments is regulated by linear Ca^{2+} pumps and leaks. After modifying the store to include a $[Ca^{2+}]_i$-sensitive leak, the model also exhibits oscillations such as those observed experimentally. The model was tested by comparing measured and predicted net Ca^{2+} fluxes during the oscillatory cycle. Three independent fluxes were measured, describing the rates of 1) Ca^{2+} entry across the plasma membrane, 2) Ca^{2+} release by the internal store, and 3) Ca^{2+} extrusion across the plasma membrane and uptake by the internal store. Starting with estimates of the model parameters deduced from post-stimulus relaxations and the rapid upstroke, a set of parameter values was found that provides a good description of $[Ca^{2+}]_i$ throughout the oscillatory cycle. With the same parameter values, there was also good agreement between the measured and simulated net fluxes. Thus, a one-pool model with a single $[Ca^{2+}]_i$-sensitive Ca^{2+} permeability is adequate to account for many of the quantitative properties of steady-state $[Ca^{2+}]_i$ oscillations in sympathetic neurons. Inactivation of the intracellular Ca^{2+} permeability, cooperative nonlinear Ca^{2+} uptake and extrusion mechanisms, and functional links between plasma membrane Ca^{2+} transport and the internal store are not required.

INTRODUCTION

$[Ca^{2+}]_i$ oscillations have been described in a variety of cells (for reviews, see Tsien and Tsien, 1990; Jacob, 1990a; Tepikin and Petersen, 1992; Fewtrell, 1993; Berridge, 1993; Hille et al., 1994). There appear to be multiple mechanisms. In some cells, oscillations reflect periodic depolarization and increased Ca^{2+} entry across the plasma membrane. In others, oscillations are dominated by uptake and release by internal stores. This study focuses on caffeine-induced $[Ca^{2+}]_i$ oscillations in bullfrog sympathetic neurons, an example where oscillations reflect both Ca^{2+} transport across the plasma membrane and uptake and release by internal stores (Friel and Tsien, 1992b). These cells respond to caffeine under mildly depolarizing conditions with oscillatory changes in $[Ca^{2+}]_i$ of period ~60 s and amplitude ~200–400 nM. The oscillations are robust, in some cells lasting several hours, and are slow enough so that spatial gradients of $[Ca^{2+}]_i$ within the cytosol are probably not important to the underlying mechanism (Hernandez-Cruz et al., 1990; Hua et al., 1993). The oscillations were first described by Kuba and Nishi (1976) in terms of periodic membrane hyperpolarizations that occur when cells are exposed to caffeine. These authors concluded that the hyperpolarizations reflect periodic elevations in $[Ca^{2+}]_i$ arising from Ca^{2+}-induced Ca^{2+} release (CICR) and the subsequent activation of a Ca^{2+}-sensitive K^+ conductance. Lipscombe et al. (1988) showed that under certain conditions, caffeine does indeed elicit $[Ca^{2+}]_i$ oscillations.

Several general observations provide insight into caffeine-induced $[Ca^{2+}]_i$ oscillations (Friel and Tsien, 1992b). 1) They are not induced by depolarization alone and are seen in only a small fraction of intact cells (~5%) after exposure to caffeine alone, but are almost invariably observed when caffeine exposure and depolarization are combined. This suggests that a caffeine-sensitive mechanism is critical for the oscillations, and that membrane depolarization increases the reliability with which they occur. 2) Oscillations occur at a steady membrane potential, indicating that they do not reflect voltage-dependent changes in ion channel activity within the plasma membrane. 3) The oscillations are blocked by ryanodine (1 μM), suggesting that they require CICR via ryanodine-sensitive Ca^{2+} release channels. 4) Ca^{2+} entry from the extracellular medium influences all phases of the oscillatory cycle, but the rapid upstroke is dominated by Ca^{2+} release from an internal store. Based on these observations, a model has been proposed that describes how the net fluxes of Ca^{2+} across the plasma membrane (J_{io}) and between the cytosol and store (J_{is}) change with time during the oscillatory cycle (Friel and Tsien, 1992b).

This study extends the previous one by examining the net Ca^{2+} fluxes that underlie J_{io} and J_{is}, and by presenting a quantitative model that addresses how these fluxes can together account for a periodic steady state. The model is developed using the following approach. First, it is asked how

Received for publication 20 June 1994 and in final form 3 February 1994.

Address reprint requests to Dr. David D. Friel, Dept. of Neuroscience, Case Western Reserve University, 10900 Euclid Ave., Cleveland, OH 44106. Tel.: 216-368-4930; Fax: 216-368-4650; E-mail: ddf2@po.cwru.edu.

0006-3495/95/05/1752/15 $2.00

$[Ca^{2+}]_i$ changes in response to small experimental perturbations. It is shown that as long as the perturbations are not too strong or prolonged, the resulting $[Ca^{2+}]_i$ relaxations agree with a simple one-pool model in which Ca^{2+} transport between compartments is regulated by linear Ca^{2+} pumps and leaks, an approximation that is expected to be increasingly valid as Ca^{2+} levels become low. Because the linear model cannot explain steady-state $[Ca^{2+}]_i$ oscillations, and there is evidence that the oscillations require CICR, the internal pool is modified to include a Ca^{2+} permeability that is regulated by $[Ca^{2+}]_i$. With this extension, the model can also account for steady-state $[Ca^{2+}]_i$ oscillations and the way their frequency and amplitude change with the concentrations of external Ca^{2+} ($[Ca^{2+}]_o$) and caffeine ($[caff]_o$). Using the extended model, predictions are made regarding the properties of three independent net Ca^{2+} fluxes during the oscillatory cycle, and these predictions are tested using a perturbation technique. It is found that with parameter values that provide a good quantitative description of the time course of $[Ca^{2+}]_i$ during the oscillatory cycle, the model also gives a good account of the measured Ca^{2+} fluxes.

METHODS

All the experimental procedures used in this study have been described previously (Friel and Tsien, 1992b). For fitting the model to the data, the differential equations that describe the extended compartmental model were integrated numerically using the fourth-order Runge-Kutta method (Boyce and DiPrima, 1969) on a PDP 11/23 computer. Parameter optimization was carried out using the simplex algorithm (Kowalik and Osborn, 1968). Data analysis was carried out using programs written by the author in Basic-23 (Indee Systems, Sunnyvale, CA).

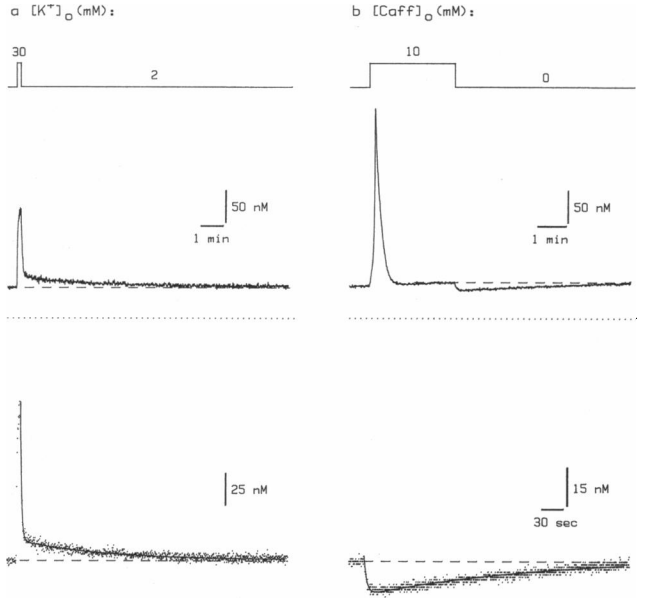

FIGURE 1 Post-stimulus $[Ca^{2+}]_i$ relaxations are biexponential with stimulus-independent time constants. (*a*) Response to brief exposure to 30 mM K^+ (*top*). The recovery is described by the sum of two decaying exponential functions (*bottom, smooth curve*) with fast and slow time constants ($\tau_{f,post\text{-}K}$, $\tau_{s,post\text{-}K}$) 3.5 and 218.2 s. Cell b141. (*b*) Response to 10 mM caffeine (*top*). The post-caffeine undershoot is described by the difference of two decaying exponential functions (*bottom, smooth curve*; note different time scales) with $\tau_{f,post\text{-}K}$ = 4.1 s and $\tau_{s,post\text{-}K}$ = 249.1 s, similar to the corresponding values for the post-K^+ recovery. The response to caffeine illustrated here was one in a series elicited to test recovery of caffeine responsiveness after a long conditioning exposure. For this response, the recovery time was brief (3.6 min) accounting for the difference from responses typically elicited by 10 mM caffeine from fully responsive cells. Dotted lines show zero $[Ca^{2+}]_i$. Cell b09s.

RESULTS

$[Ca^{2+}]_i$ relaxations after application and removal of high K^+ or caffeine

To understand why $[Ca^{2+}]_i$ oscillates under conditions of steady stimulation, it is helpful to consider first how $[Ca^{2+}]_i$ changes in response to small perturbations. Fig. 1 illustrates $[Ca^{2+}]_i$ relaxations that follow application and removal of two different stimuli, high K^+ (30 mM; Fig. 1 *a*, *top*) and caffeine (10 mM; Fig. 1 *b*, *top*). These stimuli influence Ca^{2+} transport in different ways: high K^+ causes membrane depolarization and voltage-dependent Ca^{2+} entry, whereas caffeine releases Ca^{2+} from an internal store (Friel and Tsien, 1992a). The $[Ca^{2+}]_i$ relaxations induced by these stimuli are correspondingly different: maintained exposure to 30 mM K^+ leads to a steady rise in $[Ca^{2+}]_i$, whereas caffeine only changes $[Ca^{2+}]_i$ transiently (the response illustrated in Fig. 1 *a* was elicited by brief exposure to high K^+ during which the steady state level of $[Ca^{2+}]_i$ was not reached).

It is useful to distinguish $[Ca^{2+}]_i$ relaxations that occur during exposure to high K^+ or caffeine from those that occur after the stimuli are withdrawn. While the relaxations that occur during stimulation ("on" relaxations) are often kinetically complex, presumably because they reflect $[Ca^{2+}]_i$- and time-dependent permeabilities responsible for voltage-dependent Ca^{2+} entry and CICR, the relaxations that follow stimulus removal ("off" relaxations) can be closely approximated by the sum of two decaying exponential functions, with well-resolved fast and slow components (Fig. 1, *a* and *b*, *bottom, smooth curves*). Interestingly, the post-K^+ and post-caffeine $[Ca^{2+}]_i$ relaxations are described by the same fast and slow time constants, as long as the exposure to high K^+ is brief. For example, in cells that were exposed to 30 mM K^+ for 7–12.7 s, the fast and slow time constants describing the "off" relaxations were $\tau_{f,post\text{-}K}$ = 5.5 ± 0.91 s and $\tau_{s,post\text{-}K}$ = 411.9 ± 147.2 s (N = 5, mean ± SEM). The analogous quantities describing the post-caffeine $[Ca^{2+}]_i$ undershoot were $\tau_{f,post\text{-}caff}$ = 4.1 ± 0.4 s and $\tau_{s,post\text{-}caff}$ = 655.6 ± 131.3 s (N = 14, no significant difference between $\tau_{f,post\text{-}K}$ and $\tau_{f,post\text{-}caff}$ or between $\tau_{s,post\text{-}K}$ and $\tau_{s,post\text{-}caff}$, $p > 0.1$).

The fast and slow relaxation time constants were fairly consistent for a given cell and method of perturbation, but there was considerable variability between cells. To determine whether this variability might have obscured a dependence of the time constants on the method of stimulation, post-K^+ and post-caffeine relaxation time constants were compared in individual cells. Trial-to-trial variability in the measured time constants prompted a comparison between the distributions of $\tau_{f,post\text{-}K}$ and $\tau_{f,post\text{-}caff}$, and of $\tau_{s,post\text{-}K}$ and

$\tau_{s,post\text{-}caff}$. This was difficult because long and stable recordings were required to obtain samples of the τ values. In one cell for which this comparison was successfully made, $\tau_{f,post\text{-}K} = 2.7 \pm 1.1$ s, $\tau_{f,post\text{-}caff} = 2.1 \pm 1.1$ s, and $\tau_{s,post\text{-}K} = 572.2 \pm 253.6$ s, $\tau_{s,post\text{-}caff} = 226.7 \pm 44.4$ s (mean $\pm$ SD, $N = 2$ for each stimulus). It should be noted that after prolonged depolarizations, the fast time constant describing post-K^+ relaxations was somewhat longer than that measured after brief depolarization (two cells).

These results suggest that as long as the $[Ca^{2+}]_i$ elevation produced by depolarization, or the depolarization itself, is not too prolonged, the transport processes that restore the resting distribution of Ca^{2+} have no memory of the way $[Ca^{2+}]_i$ was initially perturbed. Evidently, if $[Ca^{2+}]_i$ or V_m is elevated for longer periods of time by more prolonged stimuli, some Ca^{2+} transport processes undergo changes that take many seconds to reverse.

The post-stimulus relaxations are consistent with the simplest realistic model of $[Ca^{2+}]_i$ regulation that includes an internal compartment

The characteristics of post-stimulus relaxations described above follow from the simplest realistic model of $[Ca^{2+}]_i$ regulation that can be formulated for bullfrog sympathetic neurons. This model includes three compartments: the extracellular medium (compartment o), the cytosol (i), and a single internal compartment to represent the caffeine-sensitive store (s) (see Fig. 2, *bottom right*). Other stores have not been included in the model because they do not appear to be important for the oscillations. 1) The store sensitive to carbonyl cyanide trifluoromethoxy phenylhydrazone (FCCP) plays a role in $[Ca^{2+}]_i$ regulation in sympathetic neurons when $[Ca^{2+}]_i$ is high (~500 nM; Friel and Tsien, 1994), while caffeine-induced $[Ca^{2+}]_i$ oscillations can occur at lower $[Ca^{2+}]_i$ levels. 2) The inositol 1,4,5-trisphosphate (IP_3)-sensitive store appears to have little effect on $[Ca^{2+}]_i$ regulation in these cells, judging from the magnitude of $[Ca^{2+}]_i$ responses elicited by IP_3-generating agonists (Pfaffinger et al., 1988; DDF, unpublished observations).

In formulating the model, two approximations are made initially. First, the Ca^{2+} concentration within each compartment is described by a single quantity (c_o, c_i, and c_s respectively; Fig. 2, *bottom right*). This is reasonable as long as there is little spatial variation in the Ca^{2+} concentration within compartments, and will apply if Ca^{2+} exchange within compartments is fast compared with exchange between compartments. $[Ca^{2+}]_i$ imaging studies in sympathetic neurons under whole-cell voltage clamp indicate that after a step depolarization, spatial nonuniformities in $[Ca^{2+}]_i$ dissipate within several hundred milliseconds (Hernandez-Cruz et al. 1990; Hua et al. 1993), which is fast compared with the changes in $[Ca^{2+}]_i$ that occur during the "off" relaxations (Fig. 1). Thus, during the post-stimulus relaxations, the cytosolic compartment can be regarded as "well-mixed"; it will be assumed that Ca^{2+} is distributed uniformly within the internal store as well, but this has not been tested. Second, the external medium is assumed to be large enough so that Ca^{2+} exchange between compartments i and o does not significantly influence c_o. Under these conditions, c_o can be treated as a constant; in practice, c_o is maintained by continuous superfusion (see Friel and Tsien, 1992b).

In this model, changes in c_i and c_s result from Ca^{2+} exchange between the cytosol and both the external medium and the internal compartment. Exchange is mediated by passive leaks and active pumps that generate net Ca^{2+} fluxes J_{L1}, J_{L2}, J_{P1}, and J_{P2} (dimensions: quantity of Ca^{2+} transported/time; see Fig. 2). The letter subscripts designate leak or pump fluxes, and the number subscript identifies the compartmental boundary across which transport occurs (1 = plasma membrane; 2 = store membrane). The dynamical equations describing this system are:

$$dc_i/dt = -[J_{L1} + J_{P1} + J_{L2} + J_{P2}]/v_i$$

$$dc_s/dt = [J_{L2} + J_{P2}]/v_s,$$

where v_i and v_s are the volumes of compartments i and s, respectively, and a net outward flux from the cytosol is taken as positive to conform with electrophysiological convention.

Little more can be said about the behavior of this model until the fluxes are defined. To begin, the simplest realistic definition for the net fluxes will be assumed in which each flux is proportional to c_i and c_s in the following way:

$$J_{L1} = k_{L1}(c_i - c_o) \qquad (Ca^{2+} \text{ entry})$$

$$J_{P1} = k_{P1}c_i \qquad (Ca^{2+} \text{ extrusion})$$

$$J_{L2} = k_{L2}(c_i - c_s) \qquad (Ca^{2+} \text{ release})$$

$$J_{P2} = k_{P2}c_i \qquad (Ca^{2+} \text{ uptake}),$$

where k_{L1}, k_{P1}, k_{L2}, and k_{P2} are constants (dimensions: volume/time). In the following it will be convenient to use the new rate constants $\kappa_{L1} = k_{L1}/v_i$, $\kappa_{P1} = k_{P1}/v_i$, $\kappa_{L2} = k_{L2}/v_s$, $\kappa_{P2} = k_{P2}/v_s$ (dimensions: time^{-1}). Substituting for the fluxes in the differential equations above and solving gives $c_i(t)$ and $c_s(t)$ each as a sum of two decaying exponential functions and a steady-state solution (see Appendix). The time constants ($\tau^{\pm}$) and the steady-state solutions ($c_{i,ss}$, $c_{s,ss}$) depend only on the prevailing rate parameters, v_s/v_i (= γ) and c_o, whereas the scaling factors ($\alpha_i^{\pm}$,$\alpha_s^{\pm}$), which determine the contributions of the two exponential components, also depend on initial conditions.

The behavior of this system can be illustrated in either of two ways. If c_i and c_s are displaced from their steady-state values and then allowed to relax, they will both return with a biexponential time course. Alternatively, if any rate parameter is suddenly changed, both c_i and c_s will relax biexponentially to new steady-state values that reflect the new set of rate parameters. This provides a useful way to represent stimulation by high K^+ and caffeine. The effects of high K^+-induced depolarization can be modeled by a step increase in κ_{L1}, while the effects of caffeine application can be modeled by a step increase κ_{L2}. Representing activation of

voltage-gated Ca^{2+} channels by a step increase in Ca^{2+} permeability is only a crude representation, because it ignores time-dependence of Ca^{2+} channel activation and inactivation. However, modeling the effects of membrane repolarization by imposing a rapid reduction in κ_{L1} is realistic, because repolarization is fast compared with the subsequent decline in $[Ca^{2+}]_i$ (Friel and Tsien, 1992a) and Ca^{2+} channels close rapidly with repolarization (Jones and Marks, 1989). Therefore, this should provide a reasonable description of the plasma membrane Ca^{2+} permeability after $[K^+]_o$ is lowered from 30 to 2 mM. Similarly, modeling the effects of caffeine application by a step increase in κ_{L2} almost certainly oversimplifies the action of caffeine, but a step reduction in κ_{L2} is expected to give a first approximation to the effects of caffeine removal.

Fig. 2 illustrates simulated changes in c_i and c_s that follow step changes in κ_{L1} and κ_{L2} based on the linear model described above. A step increase in κ_{L1} (*a*) leads to a biexponential rise in both c_i and c_s toward new elevated steady-state levels. A step increase in κ_{L2} (*b*) leads to Ca^{2+} release by the internal compartment and a transient rise in c_i. The "on" relaxations resemble the observed responses to high K^+ and caffeine, but only qualitatively, as revealed most clearly by comparing simulated and observed responses to caffeine. After returning κ_{L1} to its original value (*a*), c_i and c_s both decline monotonically to their resting values (*a*), whereas restoring κ_{L2} to its original value (*b*) leads to a rise in c_s as the internal compartment refills, and a transient c_i undershoot (*b*). In contrast to the "on" relaxations, the simulated "off" relaxations closely resemble the experimentally observed ones: in each case the relaxations are biexponential with the same fast and slow time constants.

These results demonstrate that the simple linear model accounts for the qualitative properties of the "on relaxations" induced by high K^+ and caffeine, and quantitatively for the post-stimulus relaxations. One interpretation is that the experimentally observed "off" relaxations reflect Ca^{2+} transport systems operating within a linear range where Ca^{2+} fluxes are nearly proportional to Ca^{2+} concentration.

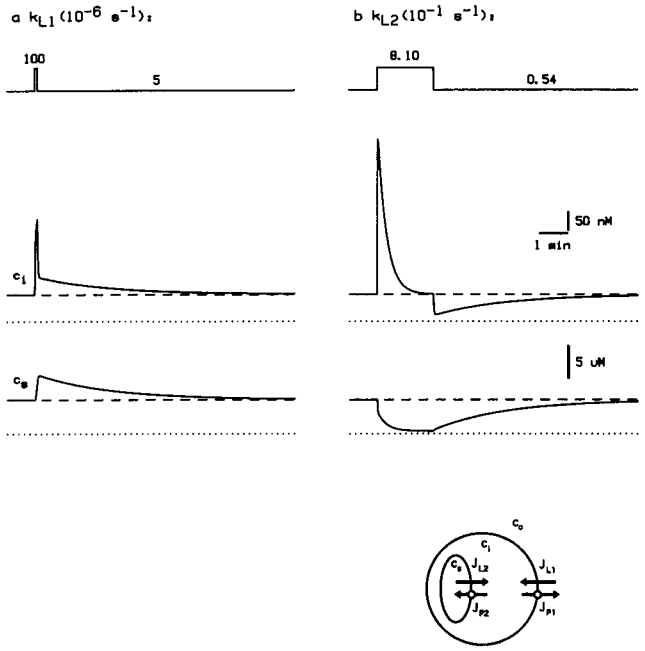

FIGURE 2 Post-stimulus $[Ca^{2+}]_i$ relaxations can be accounted for by the simplest realistic model of Ca^{2+} regulation that takes into consideration Ca^{2+} uptake and release by an intracellular compartment. Diagram depicts the two inward passive fluxes (J_{L1}, J_{L2}) and the two outward pump fluxes (J_{P1}, J_{P2}). (*a*) Brief exposure to high K^+ (as in Fig. 1 *a*) was modeled by increasing the Ca^{2+} permeability of the plasma membrane (κ_{L1}), which elicited a rise in both c_i and c_s. Lowering κ_{L1} to its original value led to a monotonic decline in both c_i and c_s to their initial values. (*b*) Exposure to caffeine (as in Fig. 1 *b*) was modeled by increasing the Ca^{2+} permeability of the store membrane (κ_{L2}), which led to a monotonic decline in c_s and a transient rise in c_i. Restoring κ_{L2} to its original level led to a monotonic rise in c_s and a transient c_i undershoot. In each case, the simulated c_i relaxations were biexponential with identical time constants for the two stimuli. Starting parameter values were (in s^{-1}): $\kappa_{L1} = 5 \times 10^{-6}$, $\kappa_{P1} = 0.132$, $\kappa_{L2} = 0.054$, $\kappa_{P2} = 3.78$. The dimensionless parameter $\gamma = 0.24$. Dashed lines indicate initial and final steady-state values, $c_{i,ss}$ and $c_{s,ss}$.

Both the "on" and "off" $[Ca^{2+}]_i$ relaxations induced by caffeine are abolished by thapsigargin

The model described above provides a simple interpretation of the $[Ca^{2+}]_i$ relaxations shown in Fig. 1. The "off" relaxation following a step reduction in κ_{L1} reflects the net loss of Ca^{2+} from the cytosol caused by Ca^{2+} extrusion across the plasma membrane, slowed by passive Ca^{2+} release from the internal compartment as it restores its initial Ca^{2+} load. The c_i undershoot initiated by a step reduction of κ_{L2} is caused by net Ca^{2+} accumulation by the internal compartment as it refills, which depresses $[Ca^{2+}]_i$ below its steady-state level. This interpretation of the post-caffeine $[Ca^{2+}]_i$ undershoot is supported by the following experimental observations (Friel and Tsien, 1992a). 1) Recovery from the undershoot after caffeine removal parallels replenishment of the store as assayed by responsiveness to caffeine. 2) Both the recovery from the undershoot and replenishment of the store are prevented by removing external Ca^{2+}. 3) After treatment with ryanodine, caffeine application fails to elevate $[Ca^{2+}]_i$, and caffeine removal fails to elicit an undershoot.

If the post-caffeine undershoot reflects Ca^{2+} uptake by the caffeine-sensitive store, then it should be eliminated by inhibiting Ca^{2+} uptake. To test this, thapsigargin (TG) was used. TG is an irreversible (or slowly reversible) inhibitor of intracellular Ca^{2+}-ATPases that accumulate Ca^{2+} into the endoplasmic reticulum (Thastrup et al., 1990). Fig. 3 *a* illustrates the protocol that was used to investigate the effects of TG on responsiveness to caffeine. Caffeine was applied while $[Ca^{2+}]_i$ was steadily elevated by exposure to 30 mM K^+. Under these conditions, caffeine produced a transient rise in $[Ca^{2+}]_i$ that was qualitatively similar to the one illustrated in Fig. 1 *b*. Also, caffeine removal elicited a biexponential $[Ca^{2+}]_i$ undershoot (see Fig. 1, *fitted smooth curve between arrows*) which, because it was more pronounced, was easier to study. A similar enhancement of the post-caffeine undershoot has been described in cardiac cells by

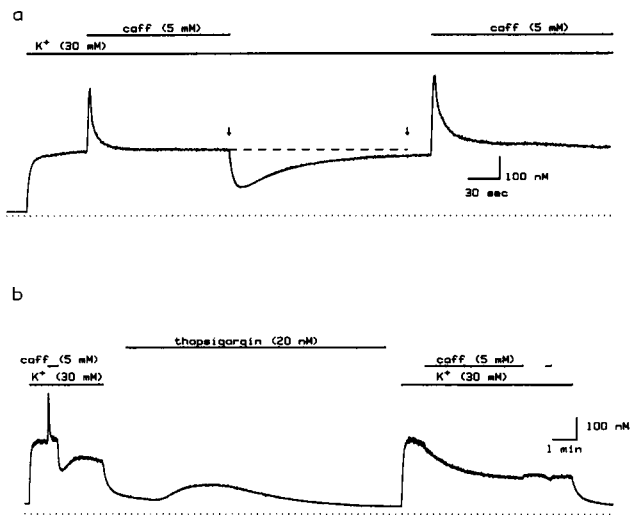

FIGURE 3 Effects of TG on responses to caffeine. (*a*) Post-caffeine $[Ca^{2+}]_i$ undershoot elicited during steady exposure to 30 mM K^+. The undershoot was well described by the sum of two decaying exponential functions with $\tau_f = 4.9$ s and $\tau_s = 50.0$ s (*superimposed curve between arrows*). Cell b12w. (*b*) Effect of TG (20 nM) on responses to caffeine application and removal during steady exposure to 30 mM K^+. TG eliminated both the caffeine-induced $[Ca^{2+}]_i$ transient and the post-caffeine undershoot. Note that after exposure to TG, caffeine lowered $[Ca^{2+}]_i$ slightly and reversibly, possibly reflecting inhibition of voltage-sensitive Ca^{2+} entry. Cell b14d.

Baro et al. (1993). Note that τ values for the post-caffeine undershoot are smaller in the presence of high K^+, possibly reflecting a dependence of Ca^{2+} transport rates on V_m, $[K^+]_o$, or $[Ca^{2+}]_i$. Note also that maintained exposure to caffeine during steady depolarization leads to $[Ca^{2+}]_i$ oscillations (e.g., Fig. 4 a, *top*).

TG (20 nM) produced a slow transient rise in $[Ca^{2+}]_i$ (Fig. 3 *b*), presumably reflecting inhibition of Ca^{2+} uptake by internal stores and an unopposed Ca^{2+} leak that gradually discharged them. The absence of an elevated steady-state $[Ca^{2+}]_i$ level after treatment with TG argues that depletion of TG-sensitive Ca^{2+} stores does not raise the Ca^{2+} permeability of the plasma membrane in sympathetic neurons (cf. Putney, 1990; Hoth and Penner, 1992; Zweifach and Lewis, 1993). After treatment with TG, high K^+ again elicited a rise in $[Ca^{2+}]_i$, but caffeine responsiveness was lost: caffeine application no longer elevated $[Ca^{2+}]_i$, and caffeine removal failed to elicit an undershoot. Evidently, caffeine did not elevate $[Ca^{2+}]_i$ because the store was discharged, and caffeine removal failed to depress $[Ca^{2+}]_i$ because uptake was inhibited. Note that the effects of TG on caffeine responsiveness resemble those of ryanodine (not shown). One interpretation is that both agents act by depleting the caffeine-sensitive store: TG, by inhibiting Ca^{2+} uptake (Lytton et al., 1991), ryanodine by rendering the store leaky to Ca^{2+} (Rousseau et al., 1987). Inhibition of caffeine-induced Ca^{2+} release by TG suggests that the caffeine-sensitive store accumulates Ca^{2+} via a sarcoplasmic or endoplasmic reticulum Ca-ATPase (SERCA) Ca^{2+} pump (Lytton et al., 1991).

These results link the "on" and "off" relaxations induced by caffeine application and removal. Together with the observations summarized above (1–3), they indicate that the relaxations reflect reversible Ca^{2+} release and uptake by a caffeine-, ryanodine-, and TG-sensitive store. It will be argued below that the ability of the caffeine-sensitive store to raise and lower $[Ca^{2+}]_i$ about its steady-state level is one of the keys to understanding caffeine-induced $[Ca^{2+}]_i$ oscillations.

After extending the linear model to include CICR, it can account for $[Ca^{2+}]_i$ oscillations

The linear model described above provides a qualitative account of $[Ca^{2+}]_i$ relaxations after depolarization and exposure to caffeine, and a quantitative account of post-stimulus relaxations. However, it cannot account for steady-state $[Ca^{2+}]_i$ oscillations that are initiated when mildly depolarized cells are exposed to caffeine (Fig. 4 *a*). Previous work has shown that $[Ca^{2+}]_i$ oscillations in sympathetic neurons require Ca^{2+}-induced Ca^{2+} release (Kuba and Nishi, 1976; Friel and Tsien, 1992b), which was not included in the model. To include CICR, κ_{L2} was redefined as follows:

$$\kappa_{L2} = \kappa_{L2}^{(0)} + \kappa_{L2}^{(1)}/[1 + (K_{d,Ca}/c_i)^n],$$

where $\kappa_{L2}^{(0)}$, $\kappa_{L2}^{(1)}$, $K_{d,Ca}$, and n are constants. $\kappa_{L2}^{(1)}$ and $\kappa_{L2}^{(0)}$ define the strength of the c_i-sensitive and c_i-insensitive Ca^{2+} permeabilities of the store, $K_{d,Ca}$ gives the c_i-sensitivity of CICR, and n influences how rapidly κ_{L2} changes with c_i. With this definition, κ_{L2} increases sigmoidally with c_i, a reasonable representation of the $[Ca^{2+}]_i$ dependence of open probability for neuronal Ca^{2+} release channels within the physiological range of $[Ca^{2+}]_i$ (Bezprozvany et al., 1991). With this definition, the system of equations describing c_i and c_s becomes nonlinear. Note that the precise definition of κ_{L2} is not important for the conclusions that follow, only that it increases sufficiently rapidly with c_i. Note also that κ_{L2} adjusts instantaneously to changes in c_i and does not inactivate (cf. Gyorke and Fill, 1993).

With this extension, the scheme can account for many of the properties of $[Ca^{2+}]_i$ oscillations that are observed when cells are exposed to caffeine under depolarizing conditions (Fig. 4 *a*). As before, exposure to high K^+ is modeled by a step increase in κ_{L1}, but treatment with caffeine is modeled by a drop in $K_{d,Ca}$ (Fig. 4 *b*), since caffeine appears to increase the $[Ca^{2+}]_i$ sensitivity of Ca^{2+} release channel gating (Rousseau et al., 1988; Rousseau and Meissner, 1989). Stepping κ_{L1} leads to a rise in c_i toward a new steady-state level (Fig 4 *b*, *dashed line*), while a subsequent reduction in $K_{d,Ca}$ leads to a transient rise in c_i followed by c_i oscillations.

In comparing simulation and experiment, a distinction must be made between the initial and steady-state effects of stimulation. The model is not expected to account for initial changes in $[Ca^{2+}]_i$, because it was formulated using assumptions that are not valid during this time. For example, it was assumed that $[Ca^{2+}]_i$ remains low enough (<500 nM) that $[Ca^{2+}]_i$ transport by the FCCP-sensitive store can be ignored. However, this condition is not always satisfied during initial responses to caffeine, possibly contributing to the broad

caffeine-induced $[Ca^{2+}]_i$ transient and the slow approach to the periodic steady-state in Fig. 4 *a*. Also, according to the model, the properties of Ca^{2+} transport do not depend explicitly on time, an approximation that is expected to be especially poor during initial responses to stimulation. Therefore, the focus of the following discussion will be steady-state $[Ca^{2+}]_i$ oscillations. Qualitative comparisons between theory and experiment will be presented first (Figs. 4–6) using model parameters that insure an unstable steady-state but are not optimized for any particular data set. After this, quantitative agreement between model and data will be addressed (Figs. 9 and 10).

Simulated oscillations resemble those observed experimentally in a number of respects: 1) c_i oscillates about $c_{i,ss}$ (Fig. 4 *b*, *dashed line*), the steady-state level reached when κ_{L2} does not depend on c_i, much as $[Ca^{2+}]_i$ oscillates about $[Ca^{2+}]_{i,ss}$, the steady level reached after exposure to ryanodine. 2) c_i and c_s oscillate out of phase, with c_s rising in two kinetically distinct phases, consistent with changes in the Ca^{2+} content of the caffeine-sensitive store during the oscillatory cycle (Friel and Tsien, 1992b). 3) Changes in the concentration of extracellular Ca^{2+} influence oscillation frequency more than amplitude (Fig. 5). 4) Changes in $K_{d,Ca}$ influence oscillation frequency and amplitude (Fig. 6 *b*) in much the same way as changing $[caff]_o$ does (Fig. 6 *a*). For example, oscillations occur only at intermediate $K_{d,Ca}$ and $[caff]_o$, and, within the range where they occur, raising $[caff]_o$ and lowering $K_{d,Ca}$ reversibly increase frequency and lower spike amplitude.

In terms of the model, the c_o-dependence of oscillation frequency and amplitude can be accounted for as follows (see Fig. 5 *b*). Cycle period largely reflects the time required for the store to be replenished. Because this is limited by c_i, raising c_o, which elevates $c_{i,ss}$ (Fig. 5 *b*, *dashed line*) shortens the period. Spike amplitude depends on the Ca^{2+} content of the store when CICR is initiated. Raising c_o elevates average c_i and κ_{L2}, causing the store to become more leaky. This lowers c_s and the driving force for net Ca^{2+} release at the time of spike initiation, depressing the amplitude (Fig. 5 *b*).

To account for the way frequency and amplitude change with $K_{d,Ca}$ (Fig. 6 *b*), it should be noted that oscillations only occur when small changes in c_i produce significant changes

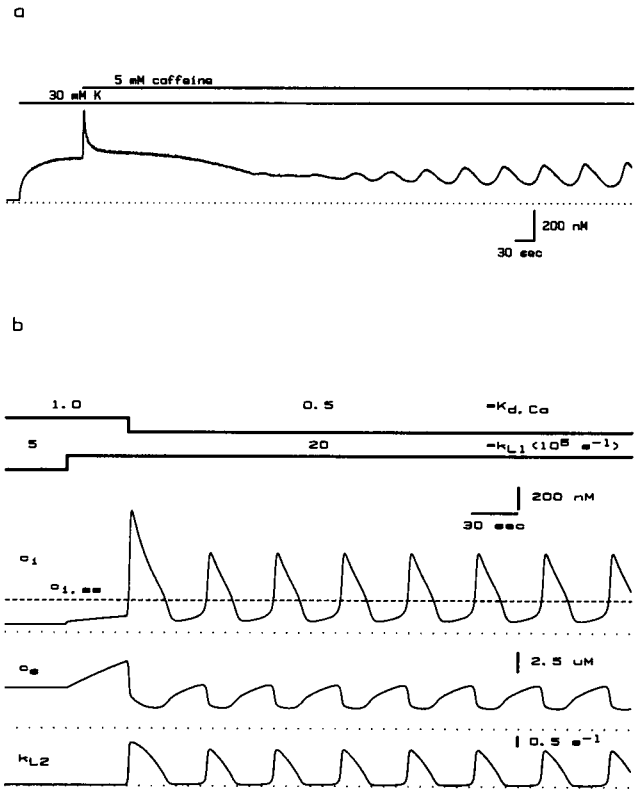

FIGURE 4 After extending the model to include a c_i-sensitive leak in the internal compartment, the model can account for steady-state oscillations. (*a*) Experimentally observed oscillations elicited by exposing a depolarized cell to caffeine (5 mM). Cell b12x (from Friel and Tsien, 1992b). (*b*) Simulated effects of depolarization and caffeine exposure on c_i, c_s, and κ_{L2}, which now varies with c_i. Note that experimentally observed oscillations can begin with a rapid onset as in the simulation (e.g., Fig. 6 *a*, *left*, where $[caff]_o$ was stepped from 1 to 5 mM, and Fig. 3 *a*, Friel and Tsien, 1992b) and that simulated oscillations can exhibit a slow onset if c_i and c_s begin near their steady-state values. Depolarization was modeled by a steady elevation of κ_{L1} (*trace*), and caffeine application was modeled by a step reduction in $K_{d,Ca}$ (*trace*). Starting parameter values were (s^{-1}): $\kappa_{L1} = 5 \times 10^{-6}$, $\kappa_{P1} = 0.132$, $\kappa_{L2}^{(0)} = 0.054$, $\kappa_{L2}^{(1)} = 2.4$, $\kappa_{P2} = 3.78$ and $K_{d,Ca} = 1$ uM, $\gamma = 0.24$, $n = 3$.

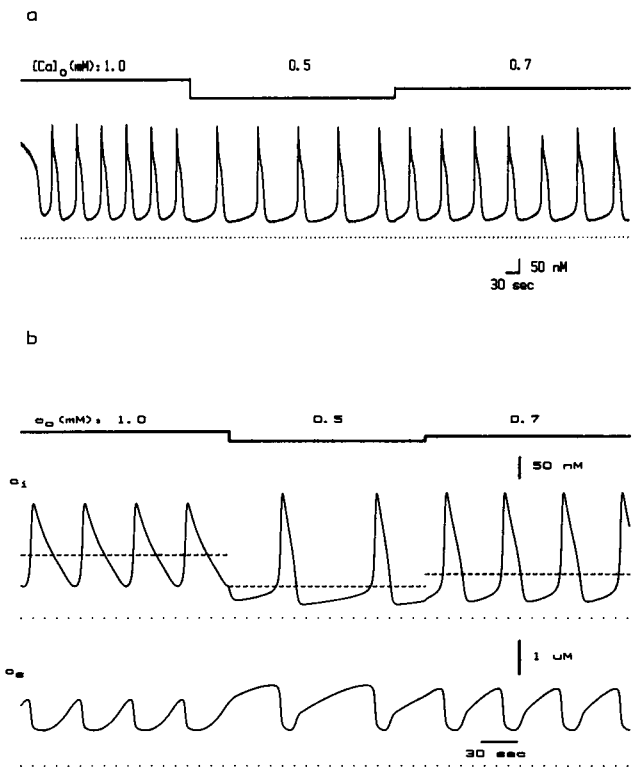

FIGURE 5 Effect of changing the concentration of external Ca^{2+} on simulated and caffeine-induced oscillations. (*a*) Experimentally observed $[Ca^{2+}]_i$ oscillations at different $[Ca^{2+}]_o$. Cell b13e (from Friel and Tsien, 1992b). (*b*) Simulated c_i oscillations at different c_o. Dashed line indicates the steady-state c_i level ($c_{i,ss}$) that would prevail in the linear model, which can be identified with $[Ca^{2+}]_{i,ss}$, the steady-state $[Ca^{2+}]_i$ level reached after $[Ca^{2+}]_i$ oscillations are inhibited by ryanodine. Unless indicated otherwise, all parameter values are the same as in Fig. 4.

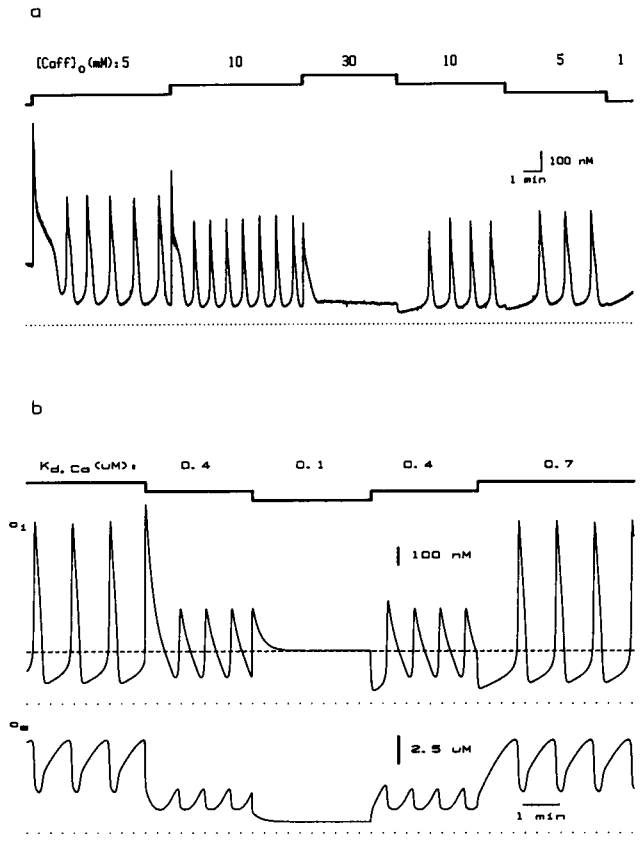

FIGURE 6 Effects of changing $K_{d,Ca}$ and $[caff]_o$ on simulated and caffeine-induced oscillations. (*a*) $[Ca^{2+}]_i$ oscillations in the presence of caffeine at different $[caff]_o$. Cell b11z (from Friel and Tsien, 1992b). (*b*) Simulated effect of changing the c_i sensitivity of CICR, $K_{d,Ca}$. Unless indicated otherwise, all parameter values are the same as in Fig. 4.

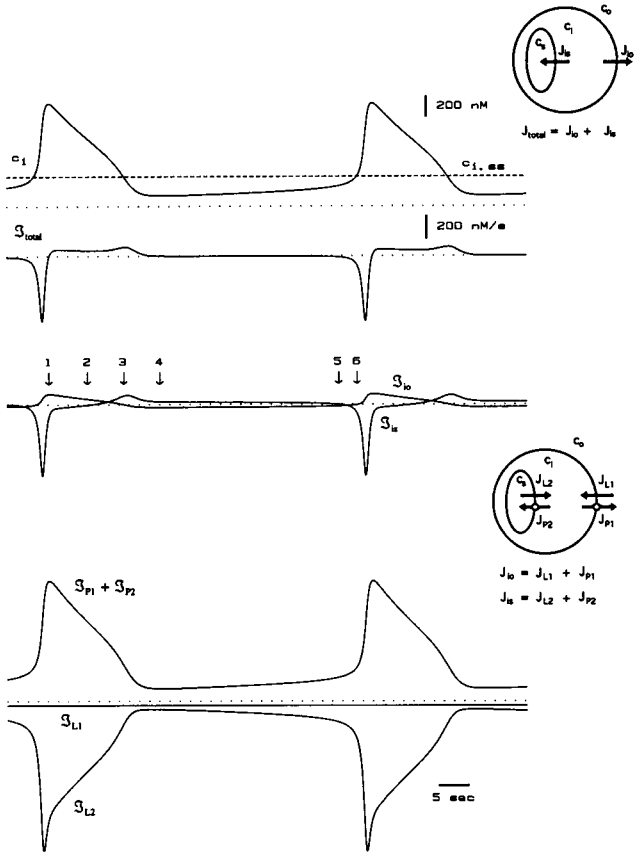

FIGURE 7 Predicted temporal properties of the Ca^{2+} fluxes that underlie $[Ca^{2+}]_i$ oscillations. The total net material flux J_{total} can be separated into J_{io} and J_{is} (*diagram, top right*; *arrows* indicate direction of positive net flux). J_{io} and J_{is} can be separated into J_{L1}, J_{P1} and J_{L2}, J_{P2} (*diagram, center right*; *arrows* indicate direction of each net flux for the parameter values used in the simulation, which are the same as those used in Fig. 4). Dividing each material flux by v_i gives the corresponding concentration fluxes (*top to bottom*): $\mathfrak{I}_{total}$, $\mathfrak{I}_{io}$ and $\mathfrak{I}_{is}$, $(\mathfrak{I}_{P1} + \mathfrak{I}_{P2})$, $\mathfrak{I}_{L1}$, and $\mathfrak{I}_{L2}$.

in κ_{L2}. If, relative to $c_{i,ss}$, $K_{d,Ca}$ is either very high (minimal activation of CICR ~ no caffeine) or very low (maximal activation of CICR ~ high caffeine), oscillations do not occur because κ_{L2} is essentially insensitive to changes in c_i, and the model reduces to the linear scheme with $\kappa_{L2} = \kappa_{L2}^{(0)}$ in the first case (no activation of CICR) and $\kappa_{L2} = \kappa_{L2}^{(0)} + \kappa_{L2}^{(1)}$ in the second (maximal activation of CICR). When $K_{d,Ca}$ is near $c_{i,ss}$, oscillations do occur, with frequency and amplitude governed by the time required for the store to refill between spikes and the driving force for net Ca^{2+} release when CICR is initiated.

Predictions regarding the underlying Ca^{2+} fluxes

The extended model makes specific predictions about the elementary fluxes that underlie changes in $[Ca^{2+}]_i$ during the oscillatory cycle. In terms of the model, $[Ca^{2+}]_i$ oscillates because the total cytosolic Ca^{2+} flux (J_{total}) is periodic, being inward (negative) during the upstroke and outward (positive) during the recovery. It is convenient to define the total concentration flux $\mathfrak{I}_{total} = J_{total}/v_i$ (Fig. 7, *second trace*). $\mathfrak{I}_{total}$ can be separated into the net Ca^{2+} flux across the plasma membrane ($\mathfrak{I}_{io} = J_{io}/v_i$) and the net flux across the store membrane ($\mathfrak{I}_{is} = J_{is}/v_i$) (Fig. 7, *middle pair of traces*). In terms of these fluxes, $\mathfrak{I}_{total}$ oscillates because there is a periodic imbalance between $\mathfrak{I}_{is}$ and $\mathfrak{I}_{io}$. $\mathfrak{I}_{total}$ is inward during the rapid upstroke, because the inward flux $\mathfrak{I}_{is}$ exceeds in magnitude the outward flux $\mathfrak{I}_{io}$. After the c_i peak, the relationship between $\mathfrak{I}_{is}$ and $\mathfrak{I}_{io}$ is reversed, with $\mathfrak{I}_{total}$ becoming an outward flux that causes c_i to decline. The model permits visualization of transitions between six critical points during the oscillatory cycle (Fig. 7, *arrows*; Friel and Tsien, 1992b). At points 1 and 4, $\mathfrak{I}_{io} = -\mathfrak{I}_{is}$, $\mathfrak{I}_{total} = 0$ and c_i is at an extreme. At points 3 and 6, $c_i = c_{i,ss}$, $\mathfrak{I}_{io} = 0$ and $\mathfrak{I}_{total} = \mathfrak{I}_{is}$. At points 2 and 5, $\mathfrak{I}_{is} = 0$ and $\mathfrak{I}_{total} = \mathfrak{I}_{io}$.

From the definitions of J_{L1} and J_{P1} above, $\mathfrak{I}_{io}$ is proportional to $(c_i - c_{i,ss})$ and tends to restore c_i to $c_{i,ss}$ after perturbations. $c_{i,ss}$ can be viewed as a "zero net flux concentration" for the plasma membrane, analogous to a reversal potential for ionic current. In terms of the model, c_i oscillates about $c_{i,ss}$ because of cycles of net Ca^{2+} release and uptake by the store, accompanied by a plasma membrane flux that tends to restore c_i to $c_{i,ss}$.

To express $\Im_{total}$ so that it can be compared with measured quantities, it is useful to rewrite dc_i/dt as follows (see Fig. 7, legend):

$$dc_i/dt = -\Im_{total} = -[\Im_{L1} + \Im_{L2} + (\Im_{P1} + \Im_{P2})],$$

the sum of three measurable concentration fluxes $\Im_{L1}$, $\Im_{L2}$, and $(\Im_{P1} + \Im_{P2})$. Before describing how these fluxes can be measured, Fig. 7 (*bottom*) illustrates their predicted behavior during the oscillatory cycle.

A few points can be made about each flux. $\Im_{L1}$ is always inward and does not change very much over the cycle. This can be understood by noting that $\Im_{L1}$ is proportional to $(c_i - c_o)$, which is always negative since $c_i < c_o$. Moreover, since c_o is larger than c_i by a factor of >1000, changes in c_i do not influence $(c_i - c_o)$ very much, so that $\Im_{L1}$ is nearly constant. $\Im_{L2}$, which is proportional to $(c_i - c_s)$, is inward as long as $c_i < c_s$ and varies periodically because of c_i-dependent changes in κ_{L2}. Finally, since $\Im_{P1}$ and $\Im_{P2}$ are both proportional to c_i, so is $(\Im_{P1} + \Im_{P2})$. Note that the total flux $\Im_{total}$ is the sum of several much larger fluxes of different sign that largely cancel one another.

Measurement of the fluxes

To determine whether the simulated time courses of $\Im_{L1}$, $\Im_{L2}$, and $(\Im_{P1} + \Im_{P2})$ resemble the actual net fluxes, it was necessary to measure them. The following method was employed (Friel and Tsien, 1992b). If an experimental perturbation rapidly changes the total net flux $\Im_{total}$ by $\Im_x$, the change in $d[Ca^{2+}]_i/dt$ immediately following the perturbation, $\Delta d[Ca^{2+}]_i/dt_{-x}$ will provide a measure of $\Im_x$. To measure $\Im_{L1}$, the initial change in $d[Ca^{2+}]_i/dt$ following rapid removal of external Ca^{2+} was determined ($\Delta d[Ca^{2+}]_i/dt_{-Ca}$), while $\Im_{L2}$ was estimated as the initial change in $d[Ca^{2+}]_i/dt$ after rapid caffeine removal ($\Delta d[Ca^{2+}]_i/dt_{-caff}$). Given $d[Ca^{2+}]_i/dt$, $\Im_{L1}$ and $\Im_{L2}$, $(\Im_{P1} + \Im_{P2})$ was calculated as follows:

$$(\Im_{P1} + \Im_{P2}) = -d[Ca^{2+}]_i/dt - (\Im_{L1} + \Im_{L2}).$$

Fig. 8 shows the effects of rapid removal of external Ca^{2+} (*a*) and caffeine (*b*) on $[Ca^{2+}]_i$ and $d[Ca^{2+}]_i/dt$ at different points in the oscillatory cycle in two different cells. As shown previously (Friel and Tsien, 1992b), Ca^{2+} removal leads to a drop in $d[Ca^{2+}]_i/dt$ that is accompanied by a fall in $[Ca^{2+}]_i$ during all phases of the cycle except the rapid upstroke. In contrast, caffeine removal leads to a decline in both $d[Ca^{2+}]_i/dt$ and $[Ca^{2+}]_i$ whenever it occurs (Fig. 8 *b*). Similar effects of caffeine removal during $[Ca^{2+}]_i$ oscillations were observed in each of six cells. Note that the slow second phase of recovery after caffeine removal is not evident on this time scale.

Comparison between measured and simulated $[Ca^{2+}]_i$ oscillations

Parameter optimization was used to determine whether the extended model can account for the detailed time courses of $[Ca^{2+}]_i$ and the measured fluxes throughout the oscillatory

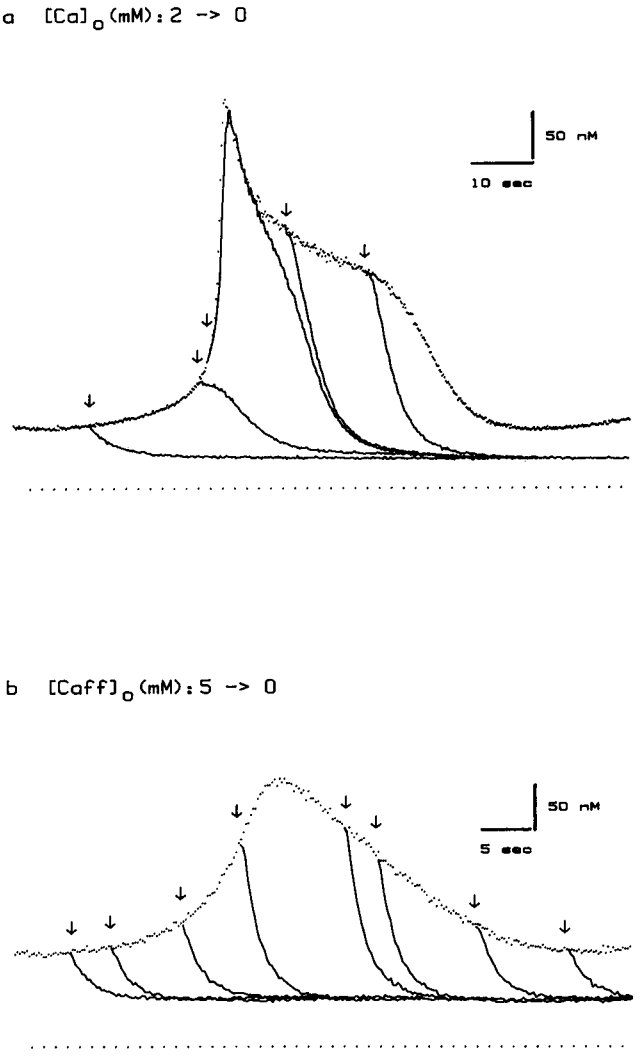

FIGURE 8 Experimental approach to measuring $\Im_{L1}$ and $\Im_{L2}$. (*a*) Rapid removal of external Ca^{2+} at different points during the oscillatory cycle (*arrows*) permits estimation of $\Im_{L1}$ in terms of the initial change in $d[Ca^{2+}]_i/dt$ ($\Delta d[Ca^{2+}]_i/dt_{-Ca}$) after Ca^{2+} removal. Cell B12z (from Friel and Tsien, 1992b). (*b*) Rapid removal of external caffeine at different points during the oscillatory cycle permits estimation of $\Im_{L2}$ as the initial change in $d[Ca^{2+}]_i/dt$ ($\Delta d[Ca^{2+}]_i/dt_{-caff}$) after caffeine removal. Cell B13u.

cycle. A parameter set was sought that minimizes $\Sigma_k(c_i(t_k) - [Ca^{2+}](t_k))^2$, where k is an index of discrete sample times. Therefore, optimization was influenced only by differences between c_i and $[Ca^{2+}]_i$. Initial estimates of the five parameters describing the linear model (κ_{L1}, κ_{P1}, $\kappa_{L2}^{(0)}$, κ_{P2}, and γ) were obtained from properties of post-stimulus $[Ca^{2+}]_i$ relaxations such as those illustrated in Fig. 1. The three additional parameters of the nonlinear model ($\kappa_{L2}^{(1)}$, $K_{d,Ca}$, and n) were estimated from the relationship between $d[Ca^{2+}]_i/dt$ and $[Ca^{2+}]_i$ during the rapid upstroke during $[Ca^{2+}]_i$ oscillations. Net fluxes were measured in the same cell to avoid complications from cell-to-cell variability.

Fig. 9 *a* (*upper panel*) shows measured $[Ca^{2+}]_i$ (*points*) and simulated c_i (*smooth curve*) over two cycles. The close agreement shows that the extended model can account for the time course of $[Ca^{2+}]_i$ during the oscillatory

cycle in this cell. The lower panel compares the measured and simulated net Ca^{2+} fluxes (*symbols* and *continuous curves*, respectively) over one cycle, with the noisy trace showing $d[Ca^{2+}]_i/dt$ ($= \Im_{total}$). It is clear that the simulated and measured net fluxes are also in reasonable agreement, even though discrepancies between measured and simulated fluxes did not explicitly influence parameter optimization. As an independent check of the linear rate laws for ($\Im_{P1} + \Im_{P2}$) and $\Im_{L1}$, the measured fluxes are plotted against $[Ca^{2+}]_i$ in Fig. 10. Over the range in which $[Ca^{2+}]_i$ oscillates, ($\Im_{P1} + \Im_{P2}$) is approximately proportional to $[Ca^{2+}]_i$, and $\Im_{L1}$ is nearly independent of $[Ca^{2+}]_i$, as expected based on the linear rate law given that $[Ca^{2+}]_i \ll [Ca^{2+}]_o$. Note that $\Im_{L1}$ did not vary appreciably with $[Ca^{2+}]_i$ in the cell shown in Fig. 9 (cf. Friel and Tsien, 1992b), possibly reflecting the lower range of $[Ca^{2+}]_i$ in this cell (<250 nM) compared with some other cells described in the previous study, where $[Ca^{2+}]_i$ reached ~400 nM.

Several differences between model and experiment can also be seen. 1) While the shape of $[Ca^{2+}]_i$ transients in many cells can be accounted for quite well by the model, in some cells the transients are somewhat more complex, characterized by a decline with more than two distinct phases (e.g., Fig. 8 *a*). 2) The simulated values of $\Im_{L1}$ systematically overestimate in magnitude the measured ones (Fig. 9, *lower panel*), while the simulated values of ($\Im_{P1} + \Im_{P2}$) slightly overestimate the measured ones when $[Ca^{2+}]_i$ is low. The basis for these discrepancies is not clear, but one contributing factor could be the restrictive assumption that each net flux is proportional to Ca^{2+} concentration. More detailed information is required concerning the time and $[Ca^{2+}]_i$ dependence of the individual net fluxes in intact cells before these issues can be addressed in detail.

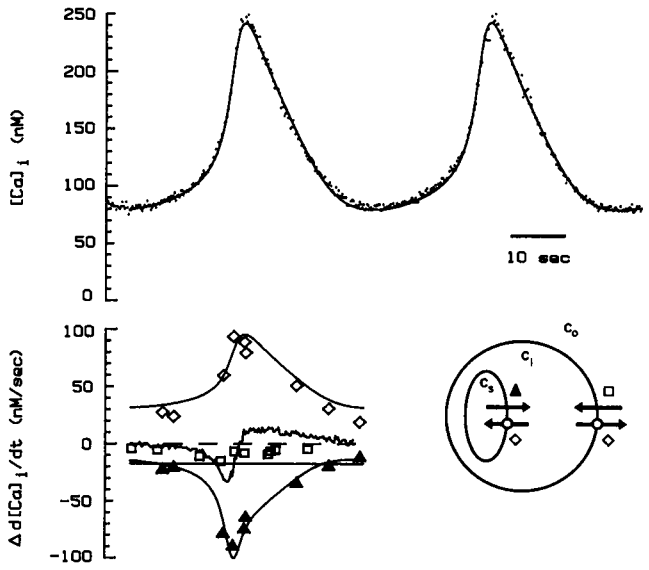

FIGURE 9 Comparison between measured and simulated Ca^{2+} fluxes. Top panel illustrates measured $[Ca^{2+}]_i$ (*points*) and simulated c_i (*smooth curve*) over two oscillatory cycles. Bottom panel shows measured $\Im_{L1}$ (□), $\Im_{L2}$ (▲), and ($\Im_{P1} + \Im_{P2}$) (◇), and the simulated values from the model (*smooth curves*). Noisy trace in lower panel is $d[Ca^{2+}]_i(t)/dt$ ($= \Im_{total}$) calculated from $[[Ca^{2+}]_i(t + \Delta t/2) - [Ca^{2+}]_i(t - \Delta t/2)]/\Delta t$, where $\Delta t = 2$ s. Parameter values for the fitted curves are: $\kappa_{L1} = 8.7 \times 10^{-6}$ s^{-1}, $\kappa_{P1} = 0.14$ s^{-1}, $\kappa_{L2}^{(0)} = 0.03$ s^{-1}, $\kappa_{L2}^{(1)} = 1.39$ s^{-1}, $\kappa_{P2} = 1.06$ s^{-1}, $K_{d,Ca} = 0.23$ μM, $n = 3.8$, $\gamma = 0.24$. Step size for the numerical integration was 150 ms.

The FCCP-sensitive store is not required for caffeine-induced $[Ca^{2+}]_i$ oscillations

Sympathetic neurons contain another Ca^{2+} store that can be defined by its sensitivity to the proton ionophore, FCCP. This store, which is thought to be mitochondrial, influences $[Ca^{2+}]_i$ responses to both membrane depolarization and caffeine if $[Ca^{2+}]_i$ approaches a high level (~500 nM) (Friel and

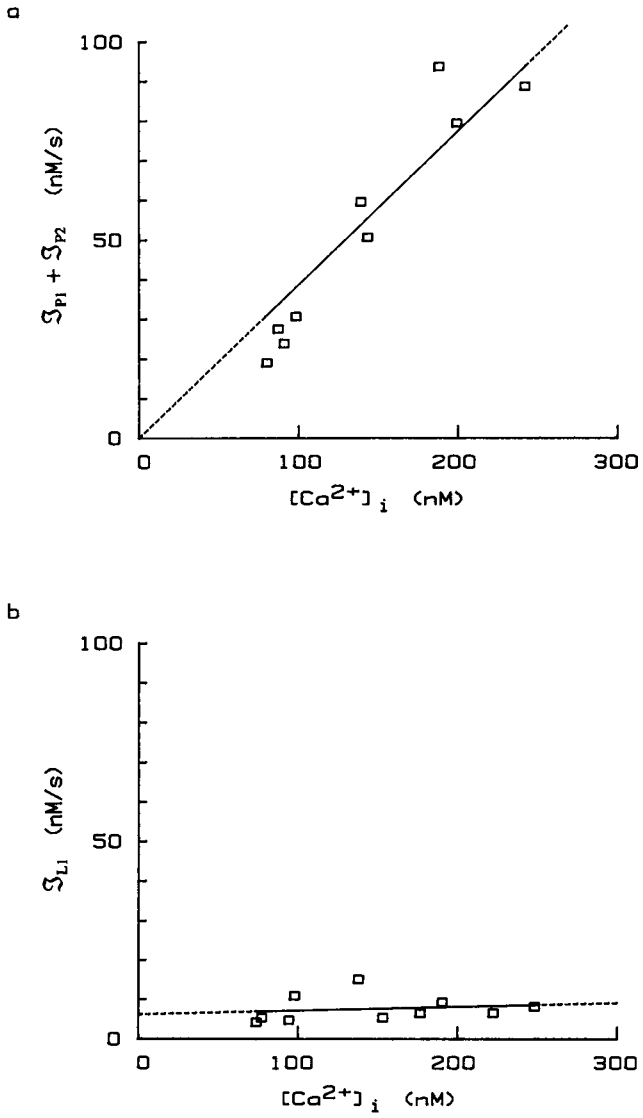

FIGURE 10 $[Ca^{2+}]_i$ dependence of $\Im_{P1} + \Im_{P2}$ (*a*) and $\Im_{L1}$ (*b*). Flux data from Fig. 9 were plotted against $[Ca^{2+}]_i$ at different points in the oscillatory cycle to assess the validity of the linear approximations: $(\Im_{P1} + \Im_{P2}) = (\kappa_{P1} + \kappa_{P2})[Ca^{2+}]_i$, $\Im_{L1} = \kappa_{L1}([Ca^{2+}]_i - [Ca^{2+}]_o) \cong -\kappa_{L1}[Ca^{2+}]_o$. Linear regression analysis gives $(\kappa_{P1} + \kappa_{P2}) = 0.387$ s^{-1}.

Tsien, 1994). To investigate whether the FCCP-sensitive store plays a role during caffeine-induced $[Ca^{2+}]_i$ oscillations, FCCP (1 μM) was applied to a cell while $[Ca^{2+}]_i$ was oscillating in the presence of 30 mM K^+ and 5 mM caffeine (Fig. 11). Under these conditions, oscillations could persist for some time (at least 11 min in this cell). In contrast, FCCP has pronounced effects on $[Ca^{2+}]_i$ responses to 50 mM K^+ after applications lasting only 10–20 seconds (D. D. Friel, unpublished observations). In the maintained presence of FCCP, oscillation frequency and amplitude gradually declined, possibly reflecting the uncoupling actions of FCCP and a decline in cellular ATP levels, with its impact on ATP-dependent transport systems. Effects of FCCP on intracellular pH cannot be excluded. After removing FCCP, the oscillation frequency returned to normal over several minutes. In another cell, oscillations faded somewhat more quickly after exposure to FCCP (~6 min). Overall, these results suggest that Ca^{2+} uptake and release by the FCCP-sensitive store are not required for caffeine-induced $[Ca^{2+}]_i$ oscillations under depolarizing conditions.

DISCUSSION

Caffeine-induced Ca^{2+} oscillations provide a good example of the interplay between Ca^{2+} transport across the plasma membrane and uptake and release by internal stores. Whereas an earlier study presented information about the relative roles of these transport pathways during $[Ca^{2+}]_i$ oscillations (Friel and Tsien, 1992b) the present study examines the underlying Ca^{2+} fluxes and the way they change with time during the oscillatory cycle. A one-pool model was presented that describes the net fluxes of Ca^{2+} across the plasma membrane (J_{io}) and between the cytosol and store (J_{is}) in terms of the imbalance between four net fluxes associated with different populations of Ca^{2+} channels and pumps. It was found that the model provides a reasonable qualitative description of $[Ca^{2+}]_i$ dynamics as long as $[Ca^{2+}]_i$ does not rise too high and Ca^{2+} transport rates change slowly enough to prevent development of large $[Ca^{2+}]_i$ gradients. The model also provides a quantitative account of post-stimulus $[Ca^{2+}]_i$ relaxations and of the kinetics of $[Ca^{2+}]_i$ during steady-state oscillations. Although measurements were not presented for each of the four net fluxes postulated to underlie changes in $[Ca^{2+}]_i$ during the oscillatory cycle, three independent combinations of these fluxes were measured and found to agree with predictions based on the model.

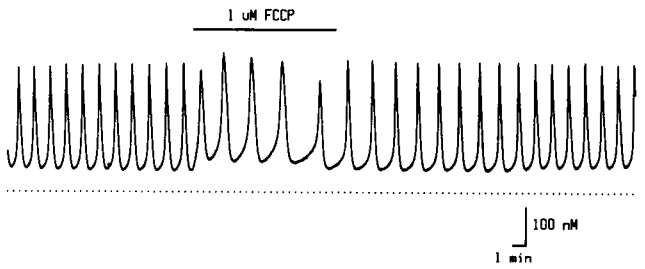

FIGURE 11 Observed effects of FCCP (1 μM) on $[Ca^{2+}]_i$ oscillations in the presence of 5 mM caffeine and 30 mM $[K^+]_o$. FCCP was dissolved in 100% ethanol to make a 10 mM solution and stored at −20°C. For each experiment, the FCCP stock solution was diluted 10,000-fold in frog Ringer's solution. Ethanol at this concentration had no detectable effect on $[Ca^{2+}]_i$ oscillations. Cell b13f.

Overview of the proposed mechanism of $[Ca^{2+}]_i$ oscillations

Based on arguments presented in Friel and Tsien (1992b), there are six critical points during the oscillatory cycle (Fig. 12, *arrows*). These points partition the cycle into intervals where $\mathfrak{I}_{io}$, $\mathfrak{I}_{is}$, and $\mathfrak{I}_{total}$ have distinct relationships. Results of the present study show how passage from one point to the next can be understood in terms of the underlying net fluxes. $\mathfrak{I}_{io}$ is the sum of the inward flux $\mathfrak{I}_{L1}$ and the outward flux $\mathfrak{I}_{P1}$, and is proportional to $(c_i - c_{i,ss})$. $\mathfrak{I}_{is}$ is the sum of the inward flux $\mathfrak{I}_{L2}$ and the outward flux $\mathfrak{I}_{P2}$. $\mathfrak{I}_{P2}$ is proportional to c_i, while $\mathfrak{I}_{L2}$ is proportional to both the driving force for net Ca^{2+} release $(c_i - c_s)$ and the Ca^{2+} permeability of the store κ_{L2}, which rises sigmoidally with c_i.

To step through the oscillatory cycle, it is convenient to start at critical point 6, where $c_i = c_{i,ss}$, $\mathfrak{I}_{io} = 0$, and c_i rises at a rate determined by the inward net flux $\mathfrak{I}_{is}$. c_i rises above $c_{i,ss}$ at increasing rate because the inward flux $\mathfrak{I}_{is}$ rises more rapidly with c_i than the outward flux $\mathfrak{I}_{io}$. In other words, Ca^{2+} is released by the store faster than it can be transported outward across the plasma membrane. The rapid rise in $\mathfrak{I}_{is}$ reflects the growing imbalance between $\mathfrak{I}_{L2}$, which rises supralinearly with c_i, and the opposing flux $\mathfrak{I}_{P2}$, which increases linearly with c_i. However, as the store loses Ca^{2+}, the driving force for Ca^{2+} release declines, causing $\mathfrak{I}_{L2}$, and therefore $\mathfrak{I}_{is}$, to decline in magnitude. When the inward flux $\mathfrak{I}_{is}$ is balanced by the outward flux $\mathfrak{I}_{io}$, $\mathfrak{I}_{total} = 0$ and c_i is maximal (point 1). It is the reduced driving force for passive Ca^{2+} release as the store becomes depleted that causes the magnitude of the inward flux $\mathfrak{I}_{is}$ to decline. This, along with the parallel rise in the outward flux $\mathfrak{I}_{io}$, is responsible for terminating the c_i rise. As $\mathfrak{I}_{is}$ continues to decline, $\mathfrak{I}_{total}$ becomes an outward net flux and c_i begins to fall. As it falls, both $\mathfrak{I}_{L2}$ and $\mathfrak{I}_{P2}$ decline, but $\mathfrak{I}_{L2}$ falls more rapidly than $\mathfrak{I}_{P2}$ owing to its strong dependence on c_i, causing $\mathfrak{I}_{is}$ to decline. When $\mathfrak{I}_{L2}$ and $\mathfrak{I}_{P2}$ are in balance, $\mathfrak{I}_{is} = 0$ and c_i declines at a rate determined exclusively by the outward flux $\mathfrak{I}_{io}$ (point 2). The continued decline in $\mathfrak{I}_{L2}$ causes $\mathfrak{I}_{is}$ to become outwardly directed, and the store starts to refill. Now, c_i falls under the influence of two outward net fluxes, $\mathfrak{I}_{io}$ and $\mathfrak{I}_{is}$. When c_i reaches $c_{i,ss}$, $\mathfrak{I}_{io} = 0$ and c_i falls at a rate determined by the outward flux $\mathfrak{I}_{is}$ (point 3).

c_i falls below $c_{i,ss}$ because the outward flux $\mathfrak{I}_{is}$ continues to exceed the inward flux $\mathfrak{I}_{io}$, i.e., Ca^{2+} is taken up by the store more rapidly than it can leak inward across the plasma membrane. As the store refills, $\mathfrak{I}_{L2}$ rises, causing $\mathfrak{I}_{is}$ to decline in magnitude. When the declining outward flux $\mathfrak{I}_{is}$ is just balanced by the rising inward flux $\mathfrak{I}_{io}$, $\mathfrak{I}_{total} = 0$ and c_i

reaches a minimum (point 4). It is the increased driving force for passive Ca^{2+} release as the store refills that causes the outward flux $\Im_{is}$ to decline. This, along with the parallel rise in the inward flux $\Im_{io}$, terminates the c_i undershoot. The continued decline in $\Im_{is}$ shifts the balance between $\Im_{io}$ and $\Im_{is}$ so that $\Im_{total}$ becomes an inward net flux and c_i starts to rise. As c_i rises, both $\Im_{L2}$ and $\Im_{P2}$ rise in magnitude, but $\Im_{L2}$ rises more rapidly than $\Im_{P2}$ owing to its sigmoidal dependence on c_i. As a result, the outward flux $\Im_{is}$ declines. When $\Im_{L2}$ and $\Im_{P2}$ are in balance, $\Im_{is} = 0$ and c_i rises at a rate determined exclusively by $\Im_{io}$ (point 5). The continued rise in $\Im_{L2}$ causes $\Im_{is}$ to become inwardly directed and c_i rises under the influence of two inward net fluxes, $\Im_{io}$ and $\Im_{is}$. Because the store is now replenished, this leads to an accelerated rise in c_i. When c_i reaches $c_{i,ss}$, $\Im_{io} = 0$ and c_i again rises at a rate determined by the inward flux $\Im_{is}$ (point 6) to initiate a new cycle.

One of the key features of this mechanism of $[Ca^{2+}]_i$ oscillations is that the store can, during certain phases of the cycle, accumulate or release Ca^{2+} so rapidly that Ca^{2+} transport across the plasma membrane cannot keep pace. However, each excursion from $c_{i,ss}$ is limited because the store cannot serve as a continuous Ca^{2+} source or sink; inactivation of the c_i-sensitive permeability is not involved. Another interesting feature of the model is the dual role of feedback in raising c_i above $c_{i,ss}$ during the upstroke, which is required for the store to discharge, and in lowering c_i below $c_{i,ss}$ during the downstroke, which is required for it to refill.

Simplications used in formulating the model

One of the surprising results of the present study is that simple features of $[Ca^{2+}]_i$ regulation can account for many features of $[Ca^{2+}]_i$ dynamics that are observed experimentally. Perhaps most surprising is the adequacy of linear approximations to the transport rate laws for Ca^{2+} entry through voltage-sensitive Ca^{2+} channels, Ca^{2+} extrusion by plasma membrane Ca^{2+} pumps, and Ca^{2+} uptake by TG-sensitive Ca^{2+} pumps.

Ca^{2+} entry

A linear rate law for Ca^{2+} entry is expected for the net flux of Ca^{2+} through voltage-dependent Ca^{2+} channels under steady-state conditions if $[Ca^{2+}]_o$ is well below the concentration that gives saturating unitary fluxes. $[Ca^{2+}]_i$ oscillations were studied while cells were exposed to high K^+ (30 mM), which steadily depolarizes the membrane potential to ~−35 mV. Using constant field theory, if channel open probability is constant, the rate of Ca^{2+} entry will be proportional to $[Ca^{2+}]_o$, close to the proposed linear rate law $J_{L1} \propto (c_i - c_o)$ if $c_o \gg c_i$. Elevations of $\Im_{L1}$ at higher levels of $[Ca^{2+}]_i$ (Friel and Tsien, 1992b) may reflect $[Ca^{2+}]_i$-dependent activity of voltage-sensitive Ca^{2+} channels like that observed in other cells (Gurney et al., 1989; McCarron et al., 1992).

Ca^{2+} extrusion

Based on available information, including the results of Na^+ removal experiments (Friel and Tsien, 1994), Ca^{2+} extrusion in sympathetic neurons appears to reflect largely Ca^{2+} transport by plasma membrane Ca^{2+} pumps. The rate of extrusion is expected to increase linearly with $[Ca^{2+}]_i$ as long as $[Ca^{2+}]_i$ is low compared with the concentration giving a half-maximal transport rate ($K_{0.5}$) and the Hill coefficient does not differ greatly from one. This is found in snail neurons (Tepikin et al., 1991) when $[Ca^{2+}]_i$ is within the range encountered in the present study (<~400 nM). Extrusion rates measured in the two types of neurons are in reasonable agreement. For example, in snail neurons, the Ca^{2+} extrusion rate is ~20 nM/s at $[Ca^{2+}]_i$ ~400 nM (estimated from Fig. 3 in Tepikin et al., 1991). Assuming a linear relationship between steady-state extrusion rate and $[Ca^{2+}]_i$, is comparable with the values of $\Im_{L1}$ obtained in sympathetic neurons, ~2–4 nM/s when $[Ca^{2+}]_i$ is steady at ~100 nM (Friel and Tsien, 1992b).

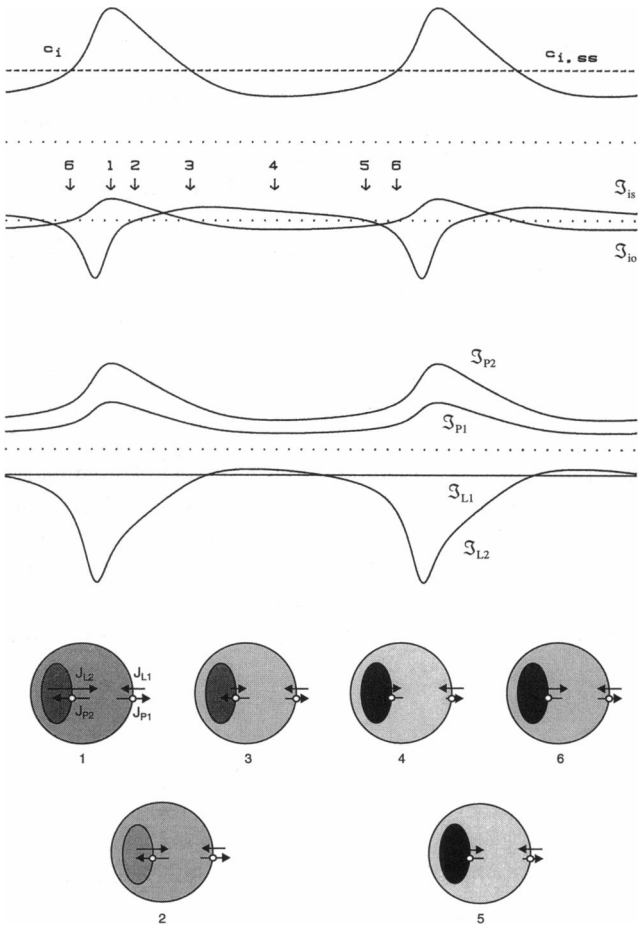

FIGURE 12 Relationship between c_i (*top*), the concentration fluxes $\Im_{io}$ and $\Im_{is}$ (second set of traces) and the fluxes that underlie them ($\Im_{L1}$, $\Im_{P1}$, $\Im_{L2}$, $\Im_{P2}$, *lower traces*) during the oscillatory cycle based on the one-pool model. Diagrams (*bottom*) illustrate the relative magnitudes of the corresponding material fluxes at six critical points (see $\Im_{io}$ and $\Im_{is}$, *arrows*). Compartmental Ca^{2+} concentrations are represented schematically by shading. Same parameter values as for the simulations in Fig. 9. Dotted lines define zero c_i and net flux.

Ca^{2+} uptake

Studies in cardiac cells have provided estimates of the $K_{0.5}$ for Ca^{2+} uptake by the sarcoplasmic reticulum of 0.3–1.0 μM with Hill coefficients of 1–1.6 (Wimsatt et al., 1990; Hove-Madsen and Bers, 1993; Balke et al. 1994). While it is difficult to extrapolate directly to the Ca^{2+} uptake system operating in sympathetic neurons, these parameters are roughly consistent with the linear approximation used in the present study. Gross departures from linearity seem unlikely, given the observed proportionality between $\Im_{P1} + \Im_{P2}$ and $[Ca^{2+}]_i$ during the oscillatory cycle (Fig. 10).

$[Ca^{2+}]_i$-sensitive Ca^{2+} release

The only nonlinear rate law in the kinetic model was used to describe $[Ca^{2+}]_i$-dependent gating of ryanodine-sensitive Ca^{2+} release channels. This was also an approximation, because the open probability of these channels varies with Ca^{2+} concentration in a bell-shaped manner (Bezprozvany et al., 1991). However, because the decline in activity occurs at very high $[Ca^{2+}]_i$ (>100 μM), the rising limb of the activity relation should provide a reasonable approximation to the $[Ca^{2+}]_i$ dependence of channel activity over the range of $[Ca^{2+}]_i$ encountered during $[Ca^{2+}]_i$ oscillations. Although time-dependent channel gating (Gyorke and Fill, 1993) was not included in the model, a possible role cannot be excluded based on available information.

Ca^{2+} buffers

Soluble Ca^{2+} buffers in either the store or cytosol can be accounted for in the model if: 1) binding equilibrium is reached rapidly compared with the rate at which intracompartmental free Ca^{2+} concentrations change during the oscillatory cycle, and 2) binding occurs with low affinity, so that for each buffer, the binding K_d is well above the prevailing free Ca^{2+} concentration. The overall effect of such buffers is to increase the effective compartmental volume (Kovacs et al., 1983). Determining whether soluble Ca^{2+} buffers in sympathetic neurons behave in this way will require additional experiments.

Interpretation of the model parameters

In terms of the model, $[Ca^{2+}]_i$ regulation in bullfrog sympathetic neurons depends on eight parameters: κ_{L1}, κ_{P1}, κ_{P2}, $\kappa_{L2}^{(1)}$, $\kappa_{L2}^{(0)}$, $K_{d,Ca}$, n, and γ, and estimates of each parameter were provided by fitting model to data. Values of $K_{d,Ca}$ (0.23 μM) and n (= 3.8) provide information about the $[Ca^{2+}]_i$ sensitivity of CICR in the presence of 5 mM caffeine. Direct interpretation of the other parameters is complicated because they depend on effective compartmental volumes. For example, κ_{L1} and κ_{P1} are the rate constants for Ca^{2+} entry and extrusion across the plasma membrane, divided by the effective cytosolic volume v_i. Similarly κ_{P2}, $\kappa_{L2}^{(1)}$, and $\kappa_{L2}^{(0)}$ are the rate constants for Ca^{2+} uptake and ($[Ca^{2+}]_i$-dependent and -independent) Ca^{2+} release by the store, divided by the store volume v_s. For each set of parameters, the effective volume depends on both the compartmental volume and the properties of intracompartmental Ca^{2+} buffers. Therefore, the lumped rate parameters do not give direct information about the transport rate constants k_{L1}, k_{P1}, $k_{L2}^{(0)}$, $k_{L2}^{(1)}$, and k_{P2}. However, independent measurements of v_i and v_s would permit calculation of the individual rate constants. In any case, the ratio k_{P1}/k_{L1} (= κ_{P1}/κ_{L1}) can be estimated from the value of resting $[Ca^{2+}]_i$. Thus, $k_{P1}/k_{L1} \sim 6.6 \times 10^3$ at 300 nM $[Ca^{2+}]_i$ ($[K^+]_o$ = 30 mM) and $\sim 2.5 \times 10^4$ at 80 nM ($[K^+]_o$ = 2 mM). In terms of the model, depolarization from $\sim$−70 to −35 mV raises the steady-state value of k_{L1}/k_{P1} ~4-fold. Based on analysis of post-stimulus $[Ca^{2+}]_i$ relaxations, the linear model provides an estimate of $k_{P2}/k_{L2}^{(0)} \sim 146$. While these estimates are undoubtedly rough, they provide a link to quantities that are, in principle, measurable.

Comparison with previous studies of $[Ca^{2+}]_i$ oscillations in sympathetic neurons

In the first study of $[Ca^{2+}]_i$ oscillations in sympathetic neurons, Kuba and Nishi (1976) described periodic membrane hyperpolarizations during exposure to caffeine. These authors concluded that the oscillations reflect periodic changes in $[Ca^{2+}]_i$ which in turn influence the activity of Ca^{2+}-activated K^+ channels in the plasma membrane. In a subsequent theoretical study, Kuba and Takeshita (1981) presented a model of $[Ca^{2+}]_i$ oscillations that emphasized the importance of Ca^{2+} transport across the plasma membrane and CICR from an internal store.

The goal of the present study was to identify which features of $[Ca^{2+}]_i$ regulation in sympathetic neurons are essential for caffeine-induced $[Ca^{2+}]_i$ oscillations, and to determine whether they can account quantitatively for the way $[Ca^{2+}]_i$ changes with time during the oscillatory cycle. The basic machinery was found in a linear three-compartment system extended to include CICR. As in previous studies, Ca^{2+} transport via Ca^{2+} pumps and leaks was included, but the corresponding transport rate laws were chosen to be as simple as possible without contradicting the existence of a stable steady-state in which $[Ca^{2+}]_i < [Ca^{2+}]_o, [Ca^{2+}]_s$. Complex transport rate laws were not invoked without experimental support from the preparation under study. For example, it was not assumed that Ca^{2+} uptake obeys a nonlinear rate law over the range of $[Ca^{2+}]_i$ where oscillations occur, and cooperative regulation of Ca^{2+} release by intraluminal Ca^{2+} was not included. Neither were required to account for the experimental observations (cf. Kuba and Takeshita, 1981; Goldbeter et al., 1990). The model was tested and shown to predict successfully the general kinetic properties of $\Im_{L1}$, $\Im_{L2}$, and ($\Im_{P1} + \Im_{P2}$) and to account for the detailed time course of these fluxes and of $[Ca^{2+}]_i$ during the oscillatory cycle.

Do $[Ca^{2+}]_i$ oscillations such as those described in the present study occur under physiological conditions?

Nishimura et al. (1991) described rhythmic membrane hyperpolarizations that occur spontaneously in neurons from intact parasympathetic ganglia. In many respects, they resemble caffeine-induced hyperpolarizations in sympathetic neurons (Kuba and Nishi, 1976): 1) external Ca^{2+} is required; 2) elevations in caffeine concentration increase the frequency; and 3) ryanodine abolishes them, although reversibly. The V_m oscillations appear to reflect periodic elevations in $[Ca^{2+}]_i$ and activation of Ca^{2+}-sensitive K^+ and Cl^- channels. Therefore, $[Ca^{2+}]_i$ oscillations such as the ones described in the present study may occur in other cells even in the absence of caffeine. While it is possible that $[Ca^{2+}]_i$ oscillations serve in the control of Ca^{2+}-sensitive processes within the cell, their role in intracellular signaling remains unclear.

Alternatively, caffeine-induced $[Ca^{2+}]_i$ oscillations in sympathetic neurons may reflect endogenous Ca^{2+} transport systems operating outside their normal operating range. According to this view, the oscillations provide insight into the transport systems that define how $[Ca^{2+}]_i$ changes under physiological conditions. Previous work has shown that both the onset and recovery of $[Ca^{2+}]_i$ responses to depolarization are slowed by ryanodine (1 μM) acting at an intracellular site (Friel and Tsien, 1992a). One interpretation is that CICR normally speeds responses to depolarization (Llano et al., 1994) and that modulation of Ca^{2+} release channel gating could tune the kinetics of responses to physiological stimuli. In this regard, it is interesting that cyclic ADP ribose has been found in a wide variety of cells (Galione, 1993) and modulates one form of the Ca^{2+} release channel (Meszaros et al., 1993) much as caffeine does (Rousseau and Meissner, 1989).

Comparison with $[Ca^{2+}]_i$ oscillations in other cells

$[Ca^{2+}]_i$ oscillations can be elicited in a variety of cells by stimuli that elevate $[IP_3]_i$ (Tsien and Tsien, 1990; Berridge, 1993). In many respects, these oscillations resemble caffeine-induced oscillations in sympathetic neurons: 1) maintained oscillations require external Ca^{2+}, and elevations in $[Ca^{2+}]_o$ raise oscillation frequency (Rooney et al., 1989); 2) oscillations are observed only at intermediate levels of stimulation, and, within the range where oscillations occur, stronger stimuli elicit higher frequency oscillations (Woods et al., 1986; Jacob et al., 1988; Rooney et al., 1989); and 3) oscillations depend on Ca^{2+} release channels whose open probability depends on $[Ca^{2+}]_i$ in a bell-shaped manner.

A number of models have been proposed to account for IP_3-induced $[Ca^{2+}]_i$ oscillations (Meyer and Stryer, 1988; Goldbeter et al., 1990; Cuthbertson and Chay, 1991; Somogyi and Stucki, 1991; DeYoung and Keizer, 1992; Dupont and Goldbeter, 1993; Atri et al., 1993; Li et al., 1994). Although it seems unlikely that one mechanism can account for all examples of $[Ca^{2+}]_i$ oscillations, it is interesting to examine formal similarities between different classes of oscillations. For example, in some cells, $[Ca^{2+}]_i$ oscillations appear to involve two distinct Ca^{2+} pools (Wakui et al., 1990). According to the two-pool model (Dupont et al., 1991; Berridge, 1991), agonist-induced elevations of $[IP_3]_i$ discharge an IP_3-sensitive store, which leads to a steady Ca^{2+} leak that produces cycles of CICR from a distinct caffeine-sensitive store. This mechanism is similar to the one described in the present study, except that the pathway controlling Ca^{2+} entry differs. While voltage-sensitive Ca^{2+} channels provide the route for Ca^{2+} entry in sympathetic neurons, different pathways appear in non-excitable cells (Putney, 1990; Jacob, 1990b; Hoth and Penner, 1992; Zweifach and Lewis, 1993; Luckhoff and Clapham, 1992).

For cells lacking a caffeine- and ryanodine-sensitive store, various one-pool models have been proposed. Most rely on the bell-shaped $[Ca^{2+}]_i$ dependence of IP_3-sensitive Ca^{2+} release channel activity (Bezprozvany et al., 1991; Finch et al., 1991), postulating that during each oscillatory cycle, $[Ca^{2+}]_i$ rises under the influence of CICR, while the $[Ca^{2+}]_i$ rise is terminated by $[Ca^{2+}]_i$-dependent inactivation of release. This would require that during the oscillatory cycle, $[Ca^{2+}]_i$ actually reaches levels that promote inactivation of IP_3-sensitive Ca^{2+} release. It is possible that this occurs in some cells but not in others. It is interesting to note that Somogyi and Stucki (1991) and Dupont and Goldbeter (1993) have developed models that, while not including $[Ca^{2+}]_i$ inactivation of IP_3-sensitive Ca^{2+} release, account for many of the features of agonist-induced $[Ca^{2+}]_i$ oscillations that are observed experimentally. In particular, the model of Somogyi and Stucki (1991) closely resembles the one described in the present study. Ultimately, evaluation of the various one-pool models of IP_3-induced $[Ca^{2+}]_i$ oscillations will require more information about $[Ca^{2+}]_i$-dependent IP_3 receptor channel gating in situ.

APPENDIX

With the rate laws for net Ca^{2+} transport given in Results, the system of dynamical equations becomes:

$$dc_i/dt = -(\kappa_{L1} + \kappa_{P1} + \gamma(\kappa_{L2} + \kappa_{P2}))c_i + \gamma\kappa_{L2}c_s + \kappa_{L1}c_o$$

$$dc_s/dt = (\kappa_{L2} + \kappa_{P2})c_i - \kappa_{L2}c_s,$$

which can be solved by standard methods (Boyce and DiPrima, 1969) to give $c_i(t)$ and $c_s(t)$:

$$c_i(t) = \alpha_i^+ e^{-t/\tau+} + \alpha_i^- e^{-t/\tau-} + c_{i,ss}$$

$$c_s(t) = \alpha_s^+ e^{-t/\tau+} + \alpha_s^- e^{-t/\tau-} + c_{s,ss}.$$

where the $\tau^{\pm}$ depend only on the elementary rate constants and γ:

$$(\tau^{\pm})^{-1} = [-[\kappa_{L1} + \kappa_{P1} + \gamma(\kappa_{L2} + \kappa_{P2}) + \kappa_{L2}]$$

$$\pm [(\kappa_{L1} + \kappa_{P1} + \gamma(\kappa_{L2} + \kappa_{P2}) + \kappa_{L2})^2 - 4\kappa_{L2}(\kappa_{L1} + \kappa_{P1})]^{1/2}]/2$$

and $\alpha_i^{\pm}, \alpha_s^{\pm}$ depend on both the rate constants and initial conditions. The steady-state solution for this system is:

$$c_{i,ss} = c_o/(1 + \kappa_{P1}/\kappa_{L1})$$

$$c_{s,ss} = c_{i,ss}(1 + \kappa_{P2}/\kappa_{L2}).$$

$c_{i,ss}$ is directly proportional to c_o and inversely proportional to $(1 + \kappa_{P1}/\kappa_{L1})$,

which depends on the ratio of κ_{P1} and κ_{L1}. $c_{s,ss}$ is proportional to $c_{i,ss}$ and (1 + κ_{P2}/κ_{L2}), which depends on the ratio of κ_{P2} and κ_{L2}.

The author would like to Drs. U. Hopfer, S. W. Jones, J. Keizer, J. Ma, and R. W. Tsien for comments on the manuscript. Some of this work was carried out in the laboratory of R. W. Tsien and was supported by a grant from the National Institutes of Health (NS07102-11).

REFERENCES

Atri, A., J. Amundson, D. Clapham, and J. Sneyd. 1993. A single pool model for intracellular calcium oscillations and waves in *Xenopus laevis* Oocyte. *Biophys. J.* 65:1727–1739.

Balke, C. W., T. M. Egan, and W. G. Wier. 1994. Processes that remove calcium from the cytoplasm during excitation-contraction coupling in intact rat heart cells. *J. Physiol.* 474:447–462.

Baro, I., S. C. O'Neill, and D. A. Eisner. 1993. Changes of intracellular [Ca^{2+}] during refilling of sarcoplasmic reticulum in rat ventricular and vascular smooth muscle. *J. Physiol.* 465:21–41.

Berridge, M. J. 1991. Cytoplasmic calcium oscillations: a two pool model. *Cell Calcium.* 12:63–72.

Berridge, M. J. 1993. Inositol trisphosphate and calcium signalling. *Nature.* 361:315–325.

Bezprozvany, I., J. Watras, and B. E. Ehrlich. 1991. Bell-shaped calcium response curves of Ins(1,4,5)P_3– and calcium gated channels from endoplasmic reticulum of cerebellum. *Nature.* 351:751–754.

Boyce, W. E., and R. C. DiPrima. 1969. Elementary Differential Equations, 2nd ed. John Wiley and Sons, New York.

Cuthbertson, K. S. R., and T. R. Chay. 1991. Modelling receptor-controlled intracellular calcium oscillators. *Cell Calcium.* 12:97–109.

De Young, G. W., and J. Keizer. 1992. A single-pool inositol 1,4,5-trisphosphate-receptor-based model for agonist-stimulated oscillations in Ca^{2+} concentration. *Proc. Natl. Acad. Sci. USA.* 89:9895–9899.

Dupont, G., M. J. Berridge, and A. Goldbeter. 1991. Signal-induced Ca^{2+} oscillations: properties of a model based on Ca^{2+}-induced Ca^{2+} release. *Cell Calcium.* 12:73–85.

Dupont, G., and A. Goldbeter. 1993. One-pool model for Ca^{2+} oscillations involving Ca^{2+} and inositol 1,4,5-trisphosphate as co-agonists for Ca^{2+} release. *Cell Calcium.* 14:311–322.

Fewtrell, C. 1993. Ca^{2+} oscillations in non-excitable cells. *Annu. Rev. Physiol.* 55:427–54.

Finch, E. A., T. J. Turner, and S. M. Goldin. 1991. Calcium as a coagonist of inositol 1,4,5-trisphosphate-induced calcium release. *Science.* 252:442–446.

Friel, D. D., and R. W. Tsien. 1992a. A caffeine and ryanodine-sensitive Ca^{2+} store in bullfrog sympathetic neurons modulates the effects of Ca^{2+} entry on [Ca^{2+}]$_i$. *J. Physiol.* 450:217–246.

Friel, D. D., and R. W. Tsien. 1992b. Phase-dependent contributions from Ca^{2+} entry and Ca^{2+} release to caffeine-induced [Ca^{2+}]$_i$ oscillations in bullfrog sympathetic neurons. *Neuron.* 8:1109–1125.

Friel, D. D., and R. W. Tsien. 1994. A FCCP-sensitive Ca^{2+} store in bullfrog sympathetic neurons and its participation in stimulus-evoked changes in [Ca^{2+}]$_i$. *J. Neurosci.* 14:4007–4024.

Galione, A. 1993. Cyclic ADP-ribose: a new way to control calcium. *Science.* 259:325–326.

Goldbeter, A., G. Dupont, and M. J. Berridge. 1990. Minimal model for signal-induced Ca^{2+} oscillations and for their frequency encoding through protein phosphorylation. *Proc. Natl. Acad. Sci. USA.* 87:1461–1465.

Gurney, A. M., P. Charnet, J. M. Pye, and J. Nargeot. 1989. Augmentation of cardiac calcium current by flash photolysis of intracellular caged-Ca^{2+} molecules. *Nature.* 341:65–68.

Gyorke, S., and M. Fill. 1993. Ryanodine receptor adaptation: control mechanism of Ca^{2+}-induced Ca^{2+} release in heart. *Science.* 260:807–809.

Hernandez-Cruz, A., F. Sala, and P. R. Adams. 1990. Subcellular calcium transients visualized by confocal microscopy in a voltage-clamped vertebrate neuron. *Science.* 247:858–862.

Hille, B., A. Tse, F. W. Tse, and W. Almers. 1994. Calcium oscillations and exocytosis in pituitary gonadotrophs. *Ann. N.Y. Acad. Sci.* 710:261–70.

Hoth, M., and R. Penner. 1992. Depletion of intracellular calcium stores activates a calcium current in mast cells. *Nature.* 355:353–356.

Hove-Madsen, L., and D. M. Bers. 1993. Passive Ca buffering and SR Ca uptake in permeabilized rabbit ventricular myocytes. *Am. J. Physiol.* 264: C677–686.

Hua, S. Y., M. Nohmi, and K. Kuba. 1993. Characteristics of Ca^{2+} release induced by Ca^{2+} influx in cultured bullfrog sympathetic neurons. *J. Physiol.* 464:245–272.

Jacob, R. 1990a. Calcium oscillations in electrically non-excitable cells. *Biochim. Biophys. Acta.* 1052:427–438.

Jacob, R. 1990b. Agonist-stimulated divalent cation entry into single cultured human umbilical vein endothelial cells. *J. Physiol.* 421:55–77.

Jacob, R., J. E. Merritt, T. J. Hallam, and T. J. Rink. 1988. Repetitive spikes in cytoplasmic calcium evoked by histamine in human endothelial cells. *Nature.* 335:40–45.

Jones, S. W., and T. N. Marks. 1989. Calcium currents in bullfrog sympathetic neurons. *J. Gen. Physiol.* 94:151–167.

Kovacs, L., E. Rios, and M. F. Schneider. 1983. Measurement and modification of free calcium transients in frog skeletal muscle fibres by a metallochromic indicator dye. *J. Physiol.* 343:161–196.

Kowalik, J., and M. R. Osborn. 1968. Methods for Unconstrained Optimization. American Elsevier, New York. 24–28.

Kuba, K., and S. Nishi. 1976. Rhythmic hyperpolarization and depolarization of sympathetic ganglion cells induced by caffeine. *J. Neurophysiol.* 39:547–563.

Kuba, K., and S. Takeshita. 1981. Simulation of intracellular Ca^{2+} oscillation in a sympathetic neuron. *J. Theor. Biol.* 93:1009–1031.

Li, Y. X., J. Rinzel, J. Keizer, and S. S. Stojilkovic. 1994. Calcium oscillations in pituitary gonadotrophs: comparison of experiment and theory. *Proc. Natl. Acad. Sci. USA.* 91,58–62.

Lipscombe, D., D. V. Madison, M. Poenie, H. Reuter, R. W. Tsien, and R. Y. Tsien. 1988. Imaging of cytosolic Ca^{2+} transients arising from Ca^{2+} stores and Ca^{2+} channels in sympathetic neurons. *Neuron* 1:355–365.

Llano, I., R. DiPolo, and A. Marty. 1994. Calcium-induced calcium release in cerebellar Purkinje cells. *Neuron.* 12:663–673.

Luckhoff, A., and D. E. Clapham. 1992. Inositol 1,3,4,5-tetrakisphosphate activates an endothelial Ca^{2+}-permeable channel. *Nature.* 355:356–358.

Lytton, J., M. Westlin, and M. R. Hanley. 1991. Thapsigargin inhibits the sarcoplasmic or endoplasmic reticulum Ca-ATP-ase family of calcium pumps. *J. Biol. Chem.* 266:17067–17071.

McCarron, J. G., J. G. McGeown, S. Reardon, M. Ikebe, F. S. Fay, and J. V. Walsh Jr. 1992. Calcium-dependent enhancement of calcium current in smooth muscle by calmodulin-dependent protein kinase II. *Nature* 357:74–77.

Meszaros, L. G., J. Bak, and A. Chu. 1993. Cyclic ADP-ribose as an endogenous regulator of the non-skeletal type ryanodine receptor Ca^{2+} channel. *Nature.* 364:76–79.

Meyer, T., and L. Stryer. 1988. Molecular model for receptor-stimulated calcium spiking. *Proc. Natl. Acad. Sci. USA* 85:5051–5055.

Nishimura, T., T. Akasu, and T. Tokimasu. 1991. A slow calcium-dependent chloride current in rhythmic hyperpolarization in neurons of the rabbit vesical pelvic ganglia. *J. Physiol.* 437:673–690.

Pfaffinger, P., M. D. Leibowitz, E. M. Subers, N. M. Nathanson, W. Almers, and B. Hille. 1988. Agonists that suppress M-current elicit phosphoinositide turnover and Ca^{2+} transients, but these events do not explain M-current suppression. *Neuron* 1:477–484.

Putney, J. W. 1990. Capacitative calcium entry revisited. *Cell Calcium* 11: 611–624.

Rooney, T. A., E. J. Sass, and A. P. Thomas. 1989. Characterization of cytosolic calcium oscillations induced by phenylephrine and vasopressin in single fura-2-loaded hepatocytes. *J. Biol. Chem.* 264:17131–17141.

Rousseau, E., J. LaDine, Q. Y. Liu, and G. Meissner. 1988. Activation of the Ca^{2+} release channel of skeletal muscle sarcoplasmic reticulum by caffeine and related compounds. *Arch. Biochem. Biophys.* 267:75–86.

Rousseau, E., and G. Meissner. 1989. Single cardiac sarcoplasmic reticulum Ca^{2+} release channel: activation by caffeine. *Am. J. Physiol.* 256:H328–H333.

Rousseau, E., J. S. Smith, G. Meissner. 1987. Ryanodine modifies conductance and gating behavior of single Ca^{2+} release channel. *Am. J. Physiol.* 253:C364–C368.

Somogyi, R., and J. W. Stucki. 1991. Hormone-induced calcium oscillations in liver cells can be explained by a simple one pool model. *J. Biol. Chem.* 266:11068–11077.

Tepikin, A. V., P. G. Kostyuk, V. A. Snitsarev, and P. V. Belan. 1991. Extrusion of calcium from a single isolated neuron of the snail *Helix pomatia*. *J. Membr. Biol.* 123:43–47.

Tepikin, A. V., and O. H. Petersen. 1992. Mechanisms of cellular calcium oscillations in secretory cells. *Biochim. Biophys. Acta.* 1137:197–207.

Thastrup, O., P. J. Cullen, B. K. Drobak, M. R. Hanley, and A. P. Dawson. 1990. Thapsigargin, a tumor promoter, discharges intracellular Ca^{2+} stores by specific inhibition of the endoplasmic reticulum Ca^{2+}-ATPase. *Proc. Natl. Acad. Sci. USA.* 87:2466–2470.

Tsien, R. W., and R. Y. Tsien. 1990. Calcium channels, stores and oscillations. *Annu. Rev. Cell Biol.* 6:715–760.

Wakui, M., Y. V. Osipchuk, and O. H. Petersen. 1990. Receptor-activated cytoplasmic Ca^{2+} spiking mediated by inositol trisphosphate is due to Ca^{2+}-induced Ca^{2+} release. *Cell.* 63:1025–32.

Wimsatt, D. K., C. M. Hohl, G. P. Brierley, and R. A. Altschuld. 1990. Calcium accumulation and release by the sarcoplasmic reticulum of digitonin-lysed mammalian ventricular cardiomyocytes. *J. Biol. Chem.* 265:14849–14857.

Woods, N. M., K. S. R. Cuthbertson, and P. H. Cobbold. 1986. Repetitive transient rises in cytoplasmic free calcium in hormone-stimulated hepatocytes. *Nature.* 319:600–602.

Zweifach, A., and R. S. Lewis. 1993. Mitogen-regulated Ca^{2+} current of T lymphocytes is activated by depletion of intracellular Ca^{2+} stores. *Proc. Natl. Acad. Sci. USA.* 90:6295–6299.